AUTONOMOUS ROBOTIC LANDMINE DETECTION, MAPPING AND AVOIDANCE

by

SANDESH GOWDA

Presented to the Faculty of the Graduate School of
The University of Texas at Arlington in Partial Fulfillment
of the Requirements
for the Degree of

MASTER OF SCIENCE IN ELECTRICAL ENGINEERING

THE UNIVERSITY OF TEXAS AT ARLINGTON

May 2015

Acknowledgements

Finally writing this page means a new hurdle is awaiting. The Master's journey has come to an end which would not be possible with the support from all the people around me.

I would like to express my sincere gratitude to my supervising professor Dr. Dan Popa for his constant guidance, motivation and financial support leading to the completion of my MS thesis. This would have not been possible without the infrastructure provided by Next Generation Systems (NGS) Lab, Univ. of Texas Arlington (UTA) and UTA Research Institute. I am grateful to my other committee professors Dr. Frank Lewis and Dr. Michael Manry for their valuable time and agreeing for my thesis defense without hesitation.

I would like to sincerely thank my parents Mr. A Kempe Gowda and Mrs. Nethravathi Gowda for their tremendous support at every step of my decision without having a second thought. And my two siblings for challenging me to keep my studies and health balance.

I would like to consider this opportunity in thanking all the NGS members for their complete patience and support on helping me get through the projects with sincere credits to Isura Ranatunga, Dr. Indika Wijayasinghe, Shweta Hardas, Sumit Kumar Das, Namrata Balakrishnan, Rommel Alonzo and Yathartha Tuladhar.

Last but not the least would like to appreciate all my friends to keep pestering me on the status of my thesis and keeping me active the whole MS program with extra-curricular activities.

April 17, 2015

Abstract

AUTONOMOUS ROBOTIC LANDMINE DETECTION,

MAPPING AND AVOIDANCE

Sandesh Gowda, MS

The University of Texas at Arlington, 2015

Supervising Professor: Dan Popa

The objective of this thesis is to develop detection algorithm to can solve socially challenging issue of Landmine mapping & removal. Landmines which used to be a safety measure during wars, play a dangerous role in civilian life, in and around the post combat regions with approximately 78 countries observing an estimate of 42 human lives killed every day. To prevent the number of casualties and manual mine clearance, mobile robots can be used for detection & mapping of the mine field region.

Mapping, detection and avoidance are the primary challenges faced on a landmine removal. In this thesis, mine center is estimated using non-linear optimization and validated through simulations for mapping. Distinguishing between the surrogate mines from the metals is accomplished using Support Vector Machine (SVM) classification, an algorithm which is formulated and validated through simulations. After detection and mapping of mines, a potential field method is employed for avoidance in simulation and incorporated the ROS (Robot Operating System) Navigation Stack on the actual robot which follows selective A* and Dijkstra's algorithm.

Results show that the Gaussian field parameter estimation localizes the mine appropriately even if the detected signals are not on the center of the mine and this is achieved through constrained non-linear optimization. This adds a repulsive force around the mine avoiding the step-over with a new navigation path generation. The SVM classifier simulations provide a clear distinguishing base line between the mines and metals based on the three channel data inputted. In future, with further anomalies into consideration, a working autonomous robot would be achieved with detection, mapping and avoidance of landmines.

Table of Contents

List of Illustrations

List of Tables

CHAPTER 1

Introduction

Laying mines in a war field is a safety procedure in protecting against intruders or enemies. Its purpose is simple – become a shield to slow down an invasion temporarily, direct attackers to kill zones, otherwise obstruct the enemies from defenseless areas.

Mines are sensitive explosives with detonating systems which can be triggered by pressure, movement, sound, magnetism and vibration. A bomb or artillery shell blowup on approaching or hitting the target while a landmine lies hidden for it to be activated by a person, animal or a vehicle's proximity. They have been characterized into anti-personnel and anti-tank mines with further addition of anti-handling technology embedded into those mines [1].

As the name suggests, anti-tank mines were built with the sole purpose of destroying military tanks. Hence, they are triggered by high pressure only; preventing them from exploding by small vehicles or pedestrians. Anti-personnel mines were/are designed to kill or injure soldiers so as to increase the opposition's logistical support. But these mines can still continue to maim and kill even after the fight is over. It is a small explosive device on or under the ground ready to detonate by pressure of a person's foot or person handling or through trip wires [1].

It is shocking to observe the sufferings caused by anti-personnel mines. According to the International Committee of the Red Cross, war surgeons tagged them the worst injuries to be treated [2]. On stepping on a blast anti-personnel mine, the blast can often rip off the legs or else with debris of soil, metal, plastic of mine casting, grass, shoes fragments, shattered bones piercing into the body wounding deeply. On similar note, if the explosion takes while handling, then the affected ligaments are fingers, hands, abdomen, spine, face and also might leave the victims blind. The anti-personnel mines

can be of the types namely – blast, fragmentation or bounding fragmentation. Fragmentation mines throw metal fragments whereas the bounding fragmentation mines are more devastating considering it jumps to a waist height and then explodes.

Thus, the victims commonly suffer permanent disability, require multiple operations, extensive rehabilitations and amputations which have social, psychological and economic consequences. Not only this, but the destruction causes the land to become dry and soil to be less fertile.

Analysis of the contribution of landmines to land degradation was conducted at University of California, Berkeley, USA, it has been stated that movement of topsoil, introduction to harmful heavy metals, rice in salt contents, decrease in organic matter content and soil crusting necessarily contribute towards land degradation [5]. It has been broadly characterized according to the below graph:

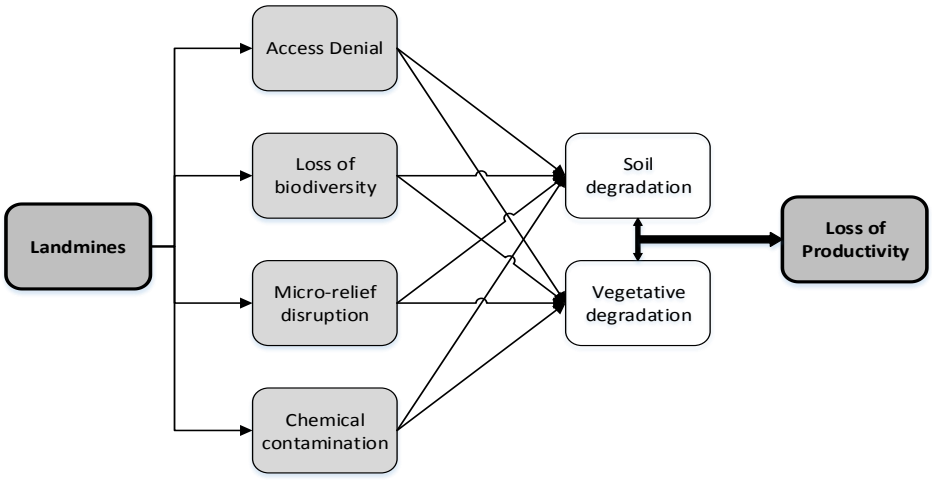

Figure 1-1 Landmine effects on Land

The categories depicted in Figure 1-1, can be defined as follows:

- Access denial: Fear of landmine presence has led to denial in the ability to use the resources available. Approximately 900 000 km2 area of land is unused due to denied access [3].

- Loss of Biodiversity: Mines have threatened various species to the edge of extinction [3].
- Micro-relief disruption: Mines causes soil instability by breaking the soil structure making it more prone to erosion [3].
- Chemical contamination: Generally the devices are composed of organic compounds like Carbon, Nitrogen, Hydrogen, Oxygen, etc. Military explosives are combinations of TNT (2, 4, 6 – trinitrotoluene), RDX (Hexogen), PETN (Nitropenta), HMX (Octogen) along with other compounds, waxes, plasticizers, stabilizers, oil, etc. These compounds percolate into ground water and soil when the mines disintegrate. These contaminants have consequences directly or indirectly to the water bodies, plants, microorganisms, soil with drinking water, food products and air. These pollutants can affect organs of fish, animals, plants and human beings which can act as a poison for their growth [3].

Obviously, landmines contribute to loss in productivity adding an adverse effect on the social and economic instability. The root problem is the landmines staying in the ground peacefully and being a hindrance for normal activity. The United Nation Mine Action Services that since 1960s more than 110 million mines have been spread across the globe and posing a threat in more than 78 countries. Approximately 15,000 to 20,000 people lose their lives by being struck by landmines and countless injured. Unarmed civilians are the primary victims of anti-personnel landmines; commonly the children, women and the elderly [4].

To eliminate the threat of mines, the only possible solution is to remove them individually without causing any damage. Anti-personnel mines costs around $3 - $30 each but neutralizing them extends from $300 to $1000 per mine depending on the mine

infected area. And even with experts disposing the mines; it is observed that for every 5000 mines extracted, one individual is killed and two injured by accidental explosions.

Accordingly at the current pace and expert's belief, for removal of such a huge number of mines, more than 1000 years would be required with no addition of mines. Blood transfusions, surgical care, fitting of orthopedic appliances for these victims are in greater need than the other war casualties.

An effort towards saving human lives and restoring the normal social, environmental and economic activity in these countries plays an important aspect for my thesis.

1.1 Existing Mine Clearing Methods

Detecting the precise location of each individual mine is the first task in clearing the landmines. Demining is a process involving surveys, mapping and minefield marking and its actual removal from the ground.

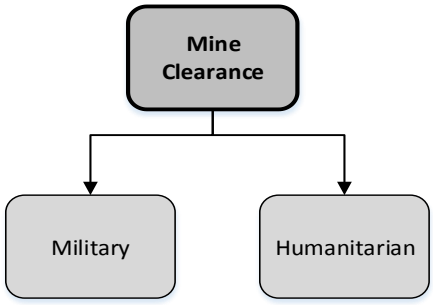

Figure 1-2 Mine clearance strategies

The **military process** just clears their strategic pathways for the soldier's movements at war which is also known as breaching, whereas **humanitarian mine clearance** is a social cause to restore peace and security at a community level. It is a challenging task to clear out the land from landmines and unexploded ordnance which

pose a danger to humanity. Once the areas are verified for public safety, the civilians can use the place without any fear or anxiety of weapons [4].

Hence the Humanitarian mine clearance phases are:

- Locating and identifying a mine field.
- Preparing the mine field for clearance operation
- Locating and marking individual mines within the identified area.
- Neutralizing the detected mines.
- Enforcing quality control measures.

According to the UN Mine Action Society [5], three main methods are operational for demining:

Manual Clearance: A trained individual with metal detectors find the mines and then they are destroyed through controlled explosion. This is a procedure where the de-miner first scans the ground with metal detector, and then uses probe to identify the signaled object to carefully uncover it. Each alarm is carefully checked for its understanding and removal. However, it's observed that one in every 1000 signals detected is a mine. It is a very slow process considering every forward movement should be thoroughly examined before risking to step ahead. Additionally, since the bullet casting and other metals might be detected using metal detectors, the false indications further delay the procedure [6] [7].

Figure 1-3 U.S. soldiers search for unexploded ordnance in Balad, Iraq [8]

The worst thing is, even if we have less casualties with professional de-miners clearing out the mine affected areas, their lives are still at stake.

Mine detection by Animals: This refers to smell based approach in combination with manual de-miners. Dogs can be 10,000 times more sensitive than man-made detector [6]. Trained dogs can detect the characteristic smell of explosive residue that emanates from the mines. Dogs do not respond towards non-explosive objects which eliminates the short comings of manual detection techniques. Terrain is not a problem for mine detection dogs and screens the land five times faster than de-miners. There are a few drawbacks to this method, such as dogs can be overwhelmed in areas of high contamination, become confused, can only work for a couple of hours and at times their effectiveness completely depends on level of training and skill of handlers. [7]

Figure 1-4 Mine detection dogs working in Vanni – National Mine Action Programme, Sri Lanka [9]

The Geneva International Center for Humanitarian Demining (GICHD) are studying the use of rodent for mine detection. Similar to dogs, African Pouched Rats can be trained to detect explosive vapors [6] [7].There are further researches carried out using rodents and can be cheapest form of landmine detector. Better sense of smell, easy maintenance, transportation and resistant to tropical disease are some advantages of using rats [10].

Figure 1-5 A pouched rat works under the rope system [10]

Mechanical Clearance: Armed bulldozers are run through the land to destroy the mines and are terrain specific, expensive and not 100% reliable. Motorized machines

designed considering the demining requirements clear the mines in its path [6]. These machines (extensions of military vehicles or armored vehicles or similar types with plows or flails) unearth the mines or explode them due to pressure. As mentioned earlier these can be used on vast areas like agricultural fields and favorable terrains with no dense vegetation [11]. But in small areas and thick vegetation areas, they are difficult to use and hence these systems tasks are reduced to maximum area coverage with verification and field clearance.

This technique is fast but has drawbacks often not destroying all the mines, burying the mines deeper, partly damaging making them vulnerable and sometimes pushing them to the sides. However, these systems along with manual efforts will smoothen the procedure of mine removal by saving time and making it safer for de-miners to concentrate on soft terrains, around trees and the residential areas.

Figure 1-6 Krohn Mechanical Mine Clearance System [11]

Krohn, shown in Figure 1-6, has been found to be capable of destroying all mines on almost any terrain freeing 30,000m^2 of land per day. Its effectiveness is becoming

10,000 times larger than manual demining with no loss and injury, according to facts certified by UN and the German government [11].

There are limited studies currently going on the effects of mine residues on the environment. But assuming the heavy machinery, there are logistical problems associated with transporting to remote areas in countries with little infrastructure and limitations of mobility and maneuverability with wheeled vehicles requiring flat terrain and tracked wheels unable to climb steep terrains. Obstacles and narrow entrances also become a problem for huge machines and hence humanitarian de-mining is now focusing in creating systems for any terrain and less logistical problems. [6] [7]

In contrast to manual methods involving humans, this research is being conducted for finding automated solutions for the demining process. Most commonly it is focused on two major aspects:1) How to reduce the de-miner casualties by use of robots and 2) Improvement of mine sensing technologies for accurate detection.

1.1.1 Robots and Humanitarian Demining

For mine removal, cost is going to be a factor – be it a human or a robot. The workers involved with de-mining will be thrilled to find out if the same job would be done remotely by using robots without the life at stake. Considering the factor that having a robot and a detector attached to it, the effectiveness should be balanced similar to manual demining.

As discussed earlier, the mechanical clearance procedure had drawbacks which can be solved by properly sized robotics solutions with suitable upgrades. This solution should be adaptable to mine field conditions improving the safety of personnel along with

efficiency, productivity and flexibility. Solving this issue of saving worker from hazardous area inherits new challenges in wide variety of fields. These include robotic mechanics and mobility, sensor and sensor fusion, autonomous or semi-autonomous navigation, and machine intelligence. Moreover, swarm robotics or a team of robots might increase the productivity for mine removal process [6].

Various humanitarian projects around the world are trying to put resources towards reliable robot platforms for demining. There are efforts on ground vehicles and air borne robots which can be tele-operated, semi-autonomous or autonomous and carry out operations of navigation, mine detection and mapping and its removal or neutralization. These operations are carried out for fast and life unthreatening causes. The research includes getting the ground platforms to have mine avoidance strategies. One concern in using robots, is its locomotion. Capability to handle varied terrain. [6]

These research options also face hindrance like designing of a universal robot for different terrains or different environmental conditions along with quality trained technicians to use the robot of high cost and sophisticated technology. Hence as an alternative mine detection and mapping through robots and its study are driving the researchers. If proven to be reliable then these can have mine removal equipment which eliminates the need for in person removal of mines. [6]

1.1.2 Mine Detection and Sensing Technologies

Demining steps cannot be carried out if location of mines are unknown. Thus, mine detection, and in general, mine sensing technologies are a major step and currently a slow process in demining. The target of technology progress is to increase the probability of the detection with low probability of false alarms. Improvements are targeted on sensor fusion and careful study of the limitations of the tools from each

location, environment and soil composition. The outcome of developing effective detection is to speed up the detection rate, reliability, accuracy and efficient distinguishing between explosives and other buried debris ensuring more safety of the de-miners and the environment. Along with the development, testing is also important to simulate the minefield conditions for real scenarios to validate the latest technology for its reliability and limitations. The procedures of actual operations in the mine field region help benchmarking the performance of the equipment, systems and the algorithms leading to enhancements.

In 2013, the IEEE Robotics and Automation Society (RAS) through a special interest group (SIGHT) started a Humanitarian project to find solutions for mine detection using robots [27]. This project called the Humanitarian Robotics and Automation Technology Challenge (HRATC) was initiated to establish an algorithm for detection, mapping and avoidance of mines [31]. The challenge gave a perspective towards use of a robot in a field filled with replica of the Anti-personnel mines. The sensing and detection of landmines from this challenge would enable the use of autonomous robots instead of manual clearance. This project became the main motivation for working on the strategy towards the optimization, neural network classification and autonomous navigation.

1.2 Contribution

This thesis involves research aimed at solving the issue of landmine detection and classification.

Proposed and validated the mine detection algorithm in simulation. The ground scan data from the 3 coils of the metal detector was collected and data analysis was carried out. The data processing involved Mine centroid estimation (nonlinear

optimization) and classification (by SVM). These techniques were validated in the Gazebo simulation environment using ROS framework.

Proposed and validated coverage algorithms with mine avoidance. For the purpose of minefield coverage, raster scanning and spiral navigation was incorporated with potential field path planning. During navigation, avoided the mines by having a repulsive field at its centroid. This is validated in the Gazebo simulation environment with the robot and simulation in MATLAB.

Experimentation with Neptune was carried out indoors for mapping, autonomous navigation and localization of the robot. To integrate the simulation results on to a real scenario, hardware & software upgrades were carried out on Neptune robot. The hardware setup included laser, camera, IMU and router fusion along with installing light-weighted Ubuntu 14.04 OS onto ADL855 PC with RTAI patch for real time driver communications and ROS Indigo. Neptune helps in mapping the environment by using SLAM g-mapping with autonomous navigation.

Awards:

Won 1st Place in HRATC competition as a part of Team Orion (Isura Ranatunga, Sandesh Gowda and Swetha Hardas), ICRA 2014. [2014 Humanitarian Robotics and Automation Technology Challenge [Humanitarian Technology]", IEEE Robotics & Automation Magazine, Volume 21, Issue 3, Sept. 2014]

The research contributions are summarized in the following papers:

- Rommel Alonzo, Sven Cremer, Sandesh Gowda, Fahad Mirza, Larry Mastromoro and Dan O Popa, "Multi-Modal Sensor and HMI Integration with

Applications in Personal Robotics", in proc. of SPIE Sensors and Technology Applications Conference, Baltimore, MD, April 2015

- Isura Ranatunga, Sandesh Gowda, Sven Cremer and Dan Popa, "Orion: Autonomous Intelligent Landmine Detection and Mapping System", (In Progress, 60% complete)

1.3 Thesis Organization

This thesis presents algorithms for mine localizing, mine detection and avoidance. It is organized as follows:

Chapter 2 discusses about different sensing technologies and research on ground and air-borne vehicles used for landmine detection.

Chapter 3 presents the hardware and software framework with the algorithms used for mine localizing, detection and avoidance with respect to the IEEE – RAS challenge.

Chapter 4 presents the simulation results for the field parameter estimator, neural network classifier and potential field technique for mine avoidance navigation technique.

Chapter 5 details the robotics platform developed and built to perform experiments of mapping and navigation with experimental results of lab mapping, avoiding a known obstacle location using potential field algorithm.

Chapter 6 summarizes the thesis and provides suggestions for future research.

CHAPTER 2

Background

Robot technologies are being applied in the hazardous fields like disaster mitigation, rescue operations, nuclear power plants, and in medical fields for support in surgical operations, nano-bots for cancer treatments, and so on [12]. Minefields also are dangerous and hence Humanitarian approach of de-mining landmines are more concerned towards the robotic usage. The procedures dealt with manual clearance, detection using animals and mechanical clearance are fruitful, however avoiding casualties or devastating the area or animals getting more prone to harmful chemical are now becoming more concerned due to the fact that there are still millions of landmines laid which needs attention. The minefield are to be seen from two perspective: one aspect being the mapping of the mines, and the other the removal of the mines. This thesis deals with first stage where current RAS-SIGHT humanitarian researchers are currently focused on using robots for mine detection. This involves three phases – detection using sensors, mapping the mines and avoidance in a minefield.

This chapter discusses the remote sensing technologies currently being worked on for improvements on mine detection. This technology can then be added on mobile platforms for autonomous performance. Further describing few of the current mobile platforms used in hazardous environments.

2.1 Remote Sensing Technology

The most demanding and challenging problems is reliable detection of the mines in all kind of terrain. Some of the sensors used for detection are ground penetrating radar, laser Doppler vibrometer, Polari-metric Infrared (IR) and hyper spectral methods, electromagnetic induction sensor - metal detector, explosive vapor detection, X-ray backscatter, and Acoustic/seismic systems uses sound or seismic waves for identifying

mines, and Electrical Impedance Tomography studies the conductivity distribution of the medium by using electric current.

2.1.1 Electromagnetic Induction sensor – Metal Detector

This sensing technology is the oldest and the most efficient method used in mine detection based on Electromagnetic Induction (EMI). The current passing through the transmit coil induces a magnetic field in the ground inducing an electric current in buried metal objects. Then the receiver coil gives an audio output on detection of the secondary weaker magnetic field created by the current from metal objects. It's more prone to high false alerts having a negative effect on the speed, cost and life. Often, demining teams uncover 100-1,000 inert metal objects for every mine (Hewish and Pengelley, 1997) [13]. To reduce the false alarms, there have been many studies carried on the EMI responses in the minefield for incorporating statistical signal processing. This approach detects and classifies, based on the independent components analysis data. [14] [15]

2.1.2 Ground Penetrating Radar (GPR)

With a manufacturing of plastic based mines to make the mine detection difficult, there came a need to use GPRs for detecting small amounts of metal being used in the evolved AP mines. The advantage is that they detect both metallic and non-metallic objects buried in the ground with an additional factor of recognizing its shape. GPRs were initially applied to study subsurface structures or buried objects in civil engineering, geology, archeology and soil and environment science. Many anti-personnel mines requires the use of large frequency signal with GPR systems. GPR helps in providing a 3D depth image of the ground. However there are limitations. For detecting small objects, high frequency signals are required for better resolution which reduces soil penetration and increases image clutter. [16]

GPR is one of the best technology for soil research. However, mine detection becomes complicated due to various reasons. The results are affected by the soil surface irregularities and the soil conditions [17]. GPR in fusion with metal detector have been very fruitful in identification of mines. Also signal processing techniques using GPR which filters out the signal for mine by nullifying the soil conditions (soil type, moisture content, and weather conditions) reduces false alarms. Few of the techniques developed are Automatic Target Recognition, methods based on 2D and 3D texture analysis, background removal, and many other statistical approach. [14]

A paper from Thomas and Glenn [18] describes the GPR based detection of mines and have tested on surrogate two types of the AP mines considering the changing parameters of radar pulse and the antenna. The Vee dipoles in a GPR using Finite-difference time-domain (FDTD) model analysis has reduced false clutters. However, with multiple reflections through rock or soil conditions, the response can sometimes be unreliable.

2.1.3 Infrared (IR) and hyper spectral methods

Mines retain or release heat at a different rate from their surroundings. Infrared methods can detect this electromagnetic radiation over the mine surface or the soil immediately over the mine. Thermal sensors are of use for identification between soil and mines based on temperature variation. This method is limited to homogeneous soil [15]. Light is the medium of data collection which makes image acquisition faster. Anthropogenic materials with the smooth surface feature can preserve polarization; allowing mine identification. Also the light scattering may be affected due to the mutation of the soil with mines present.

Thermal detection methods have also been exploited due to variations in temperature near mines compared to its surrounding; considering the fact that the mine

would be hotter during the day were as would cool off faster in the night. The discrepancy in the temperature can be removed by inducing laser illumination or microwave radiation [14]. These techniques can be applied to scan wide areas when deployed from airborne platforms and entertained for its use from a safe distance for getting alerts from the surface mines. Again its performance depends on the environment having variable response.

2.1.4 X-Ray Backscatter

This technique can create a high quality image by passing photons through mines due to its short wavelength. Although X-ray imaging on subsurface is impossible but the backscatter of X-rays can showcase buried and irradiated objects. It relies on the fact of mines and soil having the different mass densities and atomic numbers. One of the approach is collimation in which the beams and detectors are aligned for image capture but with few obstacles of increased size and weight, reduction in photons and x-ray generators. Hence this is not a feasible solution for a person handled detector. Person-portable detection is possible with un-collimated approach with x-rays covering a wide area and implementing spatial filter techniques in order to find the system response. [15]

2.1.5 Explosive Vapor Detection

The above or other mine detection techniques discuss on finding the mechanical components of the mine. Biological and chemical methods are researched further for identification of the mines. As discussed earlier in **Error! Reference source not found.** about the chemical composition of the explosives, the buried mines gradually release chemical derivatives through cracks or seams and vapor transport to the ground surface; 95% of which are absorbed by the soil surrounding it [15]. The main issue with respect to

vapor detection is its low concentrations in the air above the soil, concentrations of about few femto-grams per millimeter.

2.2 Robots in Hazardous Environments

2.2.1 Mine rescue and recovery

Mining disasters have occurred in both coal and metal/non-metal mines and involve mine rescue teams to carry out search and rescue operations in treacherous environment. To keep the rescue team safe from the hazardous condition, robots are used to assist in these underground for early reporting of the situation. In these operations, the robots may be required to move the obstacles, manipulate fan doors, and send back videos, mine gas, and temperature readings. Nominal search and rescue, mine recovery and deployments are the main tasks of underground mine rescue. First task involves inspection for human safety, second pertaining to the state of the mine for saving it or re-opening it also including environment manipulation by debris movement, opening doors or fans, etc. and thirdly the deployment of the robots since it is a crucial and urgent task for rescue operations. [19]

For operations like these, tracked or wheeled crawlers supporting highest mobility, snake robots overcome limitations of pipe crawlers and legged robots for multi-terrain ability. Wheeled robots size can range from Groundhog robot from Carnegie Mellon University (CMU) [20] to robots that can fit through pipes. And these robots can navigate underground without having issues like the snake robots whose locomotion cannot be guaranteed in these situations. For surface entry robots like V-2 as shown in Figure 2-1 (a), a wolverine variant from Mine Safety and Health Administration (MSHA) are considered for various reasons like slope entry, reliable communication, manipulator arm for handling doors or fans or remove rubbles, maneuver on rail lines or water prone areas. Similarly for borehole and void entry robots like mine cavern crawler from Inkutun

Services Ltd. which can directly start at the point of interest and has to face challenges like lowering system entry, falling rocks, transition from vertical mobility to the mine floor, debris, water and drilling foam may restrict visibility, etc.. [19]

Figure 2-1 MSHA's modified Wolverine robot, named V-2 [21]

2.2.2 Six-legged robot based system for humanitarian demining missions

A SILO6 (Spanish acronym for "six-legged locomotion system") walking robot was developed by the legged robot working group at Industrial Automation Institute (IAI) for detecting and locating unexploded ordnance. The first aim was to incorporate the legged robot technology, including electromechanical design, development, gait generation, terrain adaptation and robot teleoperation to produce an efficient robotic system for specific application of detecting and locating landmines in humanitarian missions [22]. The project was concerned with the position of the potential alarms and for

simplicity used the metal detector sensor for simplicity. For keeping the sensor at a fixed height; infrared sensors were used and Flex sensors which exhibits change in electrical resistance on external force are attached to detect objects in the metal detectors path. On detection of the suspected object, the Differential Global Positioning System (DGPS) is used for accurate localization. However, for errors like loss of satellite signals or the robot is in shadow region, the dead-reckoning system and the electromagnetic compass with extended-Kalman filter (EKF) improves robot's position. The hexapod design on SILO6 gives it a flexibility to adapt to any terrain achieving stability and energy efficient considering the insect-like and pseudo mammal-like configuration. It is semi-autonomously controlled and has an onboard controlled which receives instruction from a base station having human-machine interface for state monitoring, teleoperation and task definition. The Figure 2-2 shows the SILO6 walking robot system for potential alarms of metal ordnance. [22]

Figure 2-2 SILO6 walking robot system configured with metal detector [22]

Chapter 3

Description of Hardware and Software

This chapter discusses the hardware and software framework used for the thesis. It is related to the HRATC project with the Husky A200 robot incorporating the algorithms used in MATLAB and ROS C++ for mine localization, classification between metal signals and mine signals and the potential field technique on moving the robot towards goal points by having a repulsive force from the mine and the obstacle.

The IEEE RAS – SIGHT's mission is the application of robotics and automation technologies towards the benefit of the humanity and increasing the quality of life. This community initiated the Humanitarian Robotics and Automation Technology Challenge (HRATC) since 2013 to address the toughest problems around the globe to improve the human lives [23]. This challenge had the social cause of attempting to solve the Landmine problems as described in section 1.1. The challenge is remotely carried out in Coimbra, Portugal and in every phase of the challenge, the ROS code is delivered to the organizers for its testing. The arena is an outdoor field of 10m x 5m which is called as a minefield frame for the robots navigation.

3.1 Hardware Framework

The robot used for the challenge is a Husky A200 robot from Clearpath Robotics [24]. It is a skid steer differential drive robot. It is well equipped with sensors including laser range finder and a stereo pair of GigE cameras. The laser is mounted on a pan and tilt unit for 3D scanning of the arena which helps the user get a point cloud 3D imaging of the surrounding. The GigE cameras are used for faster data transfer over Ethernet lines with data speed of 10000Mb/s. The obstacle avoidance and navigation can be carried out using these sensors which provides all the perception required.

For its localization, the robot has RTK GPS, XSens MTi-300 IMU and Husky's odometry. GPS pinpoints its location in latitude and longitude which is converted to the minefield frame by the given UTM (Universal Transverse Mercator) Coordinate converter. IMU helps in positioning the robot using the velocity and orientation information from the accelerometer and gyro sensor. Extended Kalman filter fuses all the three positioning sensors to localize the robot in the minefield frame.

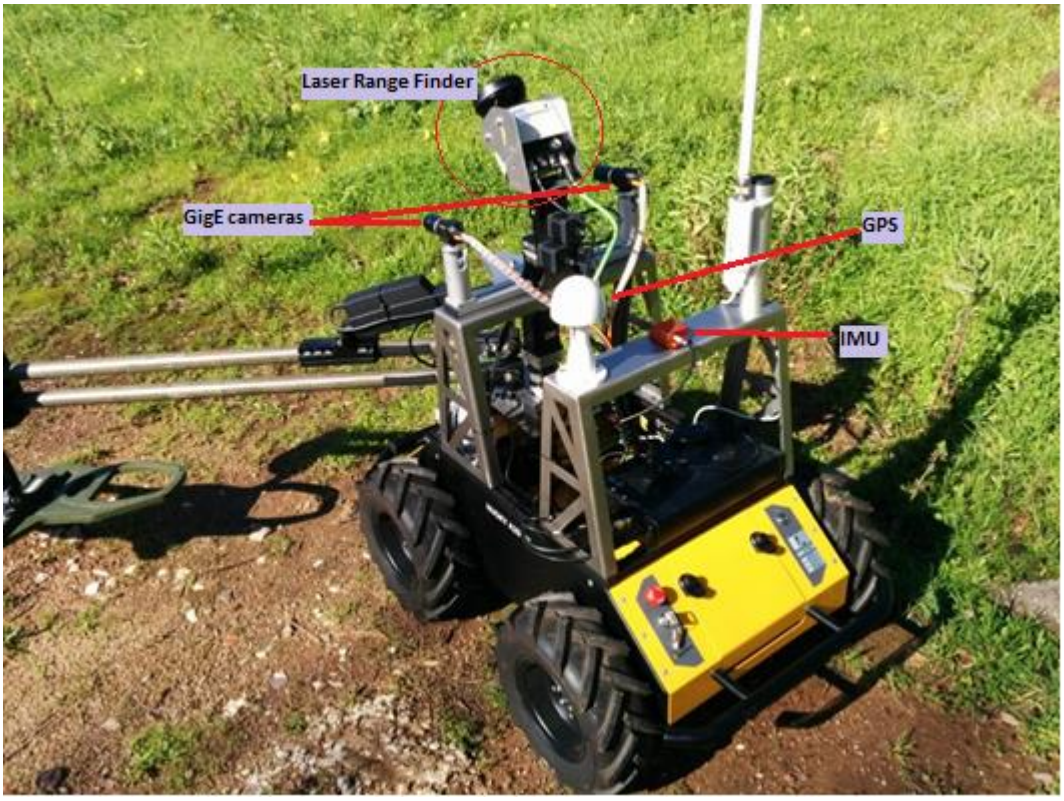

Figure 3-1 Husky A200 with all sensors for HRATC [25]

The main purpose of the robot is to detect mines. Hence a Vallon VMP3 pulse inductor metal detector shown in Figure 3-2(a) is installed on the Husky. The detector is comprised of 3 parts mainly the antenna that structures 3 coils, the rod supporting the antenna and the processing unit with 3 coil data as the input. As viewed in Figure 3-2(b), it is mounted on a 2DOF robotic arm that sweeps the detector in the front.

Figure 3-2 (a) The Vallon VMP3 metal detector (b) The VMP3 installed on the Husky robot [26]

The VMP3 detector works on pulse induction mechanism sending short and powerful current pulses through the coils. Each pulse inducing a magnetic field around the coil. An electrical spike is generated when the magnetic field reverses its polarity and collapses at the end of the pulse. Causing another current to run through the coil known

to be the reflected pulse. The duration of this pulse depends on the metal object in the vicinity of the detector. The reason is due to the fact that if there is a metallic object below the detector then an opposite magnetic field is created in the object which leads to the reflected pulse induction in the coil for a longer time. Hence, the determination of a metal object is done based on the decay length of the reflected pulse. Pulse induction mechanism helps detect metals at greater depth in comparison with other metal detector technologies. The detector is a combination of three coils outputting 3 channels of raw data along with an alarm channel. An analog switched integrator circuit evaluates these channels and are A/D converted, filtered, processed and combined to the alarm channel with a total data flow rate of 30 Hz. [26]

According to the suggestion by Vallon, a Detection Alarm with Soil Compensation can be achieved using the raw data.

$$detection_{alert} = \alpha . ch1_{data} + (1 - \alpha) . ch2_{data}$$

Where, alpha is chosen for $detection_{alert}$ to be zero for $ch1_{zero} and\ ch2_{zero}$, the response to the soil without any metal samples. Channel 1 and 2 are used for soil compensation while channel 3 (low sensitivity) can be used to get an alarm if channel 1 and 2 are overloaded. [26]

The robot runs with a robot operating system ROS framework on an Ubuntu based machine. ROS provides libraries and tools to create robot applications helping out with device driver communication, visualizations, package management, message passing, etc.

3.2 Software Framework

The first round of the HRATC was the simulator phase. A Gazebo simulator is being used for the environment setup for the minefield. The metal detector simulator was created for the action of the 2-link arm to sweep the area. A HRATC framework loads the

environment with the minefield data including the data signal related to the surrogate mines and the non-mines. The sensors included on the husky have ROS packages and their simulator helps make the environment visualization and localization same as the real scenario.

3.3 Simulation Phase Run

The challenges which became the main criteria for the mine detection are mine identification, mapping and avoidance be it the simulation phase or the real world. The below figure explains the strategy as a flowchart.

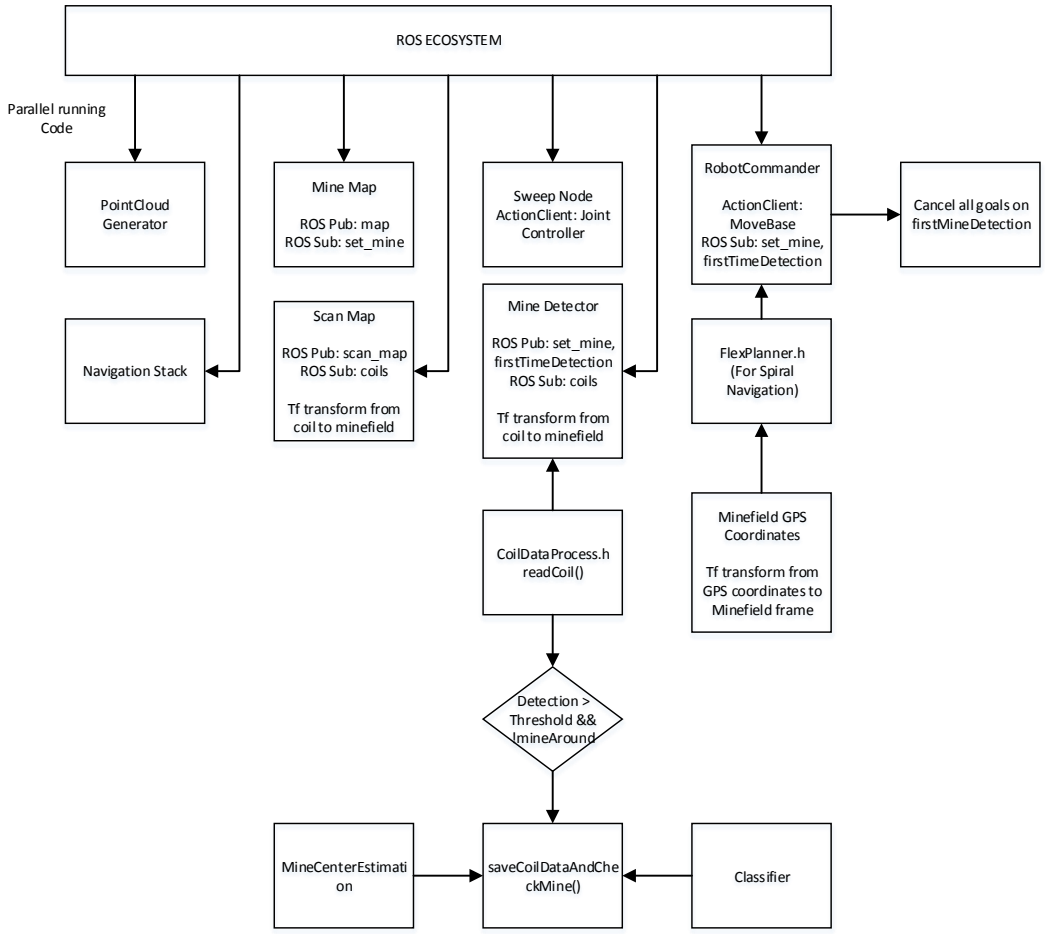

Figure 3-3 Flowchart of HRATC code in ROS

3.3.1 Mine Mapping:

Mine Mapping can be done on activating the metal detector sensor. A sweep node in the flowchart is a joint controller for the two-link metal detector arm with three coils to scan the area.

For keeping the update on the coils traced area, a **scan_map** is updated with the location of the coils while the robot is navigating. In ROS, messages can be passed easily by the help of publishing and subscribing the topics from the ROS nodes. ROS nodes are just the C++ code or python script. The C++ code subscribes to the coil

messages and transform from the coil frame of reference to the minefield frame using the transform listener node of ROS which uses the robots model transform (TF) tree. After the transformation the coils location is recorded into the image according to the resolution of the map and then a **scan_map** in the form of the occupancy grid is published for viewing purpose.

Similarly on detection of the mine signals, we have a mine_map C++ node to keep a track of the positions of the mines. It subscribes to the set_mine message is published from the mine detector node which states the location of the mine in the minefield metric frame. The location is inserted to an image specific to the resolution of the mine_map and published. Here also the static map service is updated with the mine location to consider it as an obstacle for the navigation stack which is used for the navigation around the field with obstacles.

Mines used in the competition is a metallic sphere of 1cm diameter enclosed in a plastic container which are hence called a surrogate mines. Considering all the mines to be in the form of a circle or sphere, we can estimate the signals received from the coils to be in the form of a 2D Gaussian fit; where the signal reading will the maximum at the center and reduce as we go further away from the mines. This signal detection from a sphere can be viewed as the figure below.

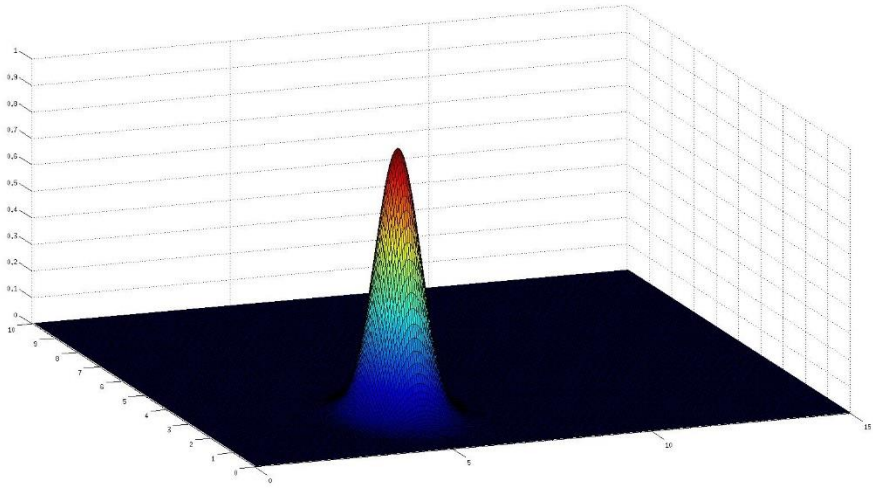

Figure 3-4 Gaussian fit for a mine center estimation

The processing of the metal detector coil readings while navigating will be able to detect a metal if the signal goes above some threshold values. In the Mine Detector node, initial mine detection is done on the basis of the threshold values. Then a Mine Center Estimation node uses a non-linear optimization using BOBYQA technique for finding the center of the mine. The test was initially carried out in matlab using the FMINCON non-linear optimization function with constrains to find the center of a Gaussian. If the initial guess is around the points where the detection alert went above the threshold values, then the error in the estimate and the actual center is negligible. This location is then published for the mine_map node to point out on the map server for avoiding it using navigation stack.

3.3.2 Mine Identification

The existence of a metal in the field is known once the detection alert value crosses a threshold. However it is important to distinguish between the surrogate mines and the metals in the field. The figure 3-5 shows the left coil – channel 1 signal of the minefield corresponding to the metal 1, metal 2 and mines placed in the area. Based on

all the channels of the coil the classification can be performed by using SVM Classifier. The classifier is trained with the mine channel inputs to output '+1' and the metals channel inputs to output '-1'. The training set for each coils is different resulting into 3 classifiers. Thus classifier outcome greater than 0.5 results into a mine identification otherwise it is a soil or a metal which is in 'Don't Care' state.

3.3.3 Obstacle and Mine Avoidance

ROS includes a navigation package which supports in the moving the mobile base around the field. This navigation stack takes the sensor data, odometry data and the goal point as the inputs and outputs safe velocity commands to the robot for its navigation from its location to the final goal point. The sensor data can be received from the camera, laser, ultrasonic, infrared, etc. In this case, we are using the laser which supports building a map and robots localization. The navigation stack accepts the sensor message in the form of LaserScan or PointCloud; sent over ROS with tf frame and time dependent information. LaserScan message is a 2D scan data with the capture of intensities along its scan points. PointCloud message stores information about the number or points in the world (a 3D view).

According to the scan points, the obstacle detection is carried out updating the map server with the obstacle points. The path planning uses this map server as an input map to move from initial point to the goal point. This path is traced using the navigation stack corresponding to the ROS trajectory planner or the DWA (Dynamic Window Approach) planner with selective Dijkstra's and A* algorithm this becoming the global planner. The local planner is the velocity commands provided to the robot to follow the global plan trajectory.

Map server is updated with respect to the sensor input data of the environment. As discussed earlier in the above sections of mapping and identification the output is the

mine location in the coordinate frame with its x and y position on processing the signals from the pulse induction metal detector sensor. An obstacle is avoided for the main reason of avoiding any damage to the environment and the robot. Here, along with the physical over ground obstacle, the underground mines is also the cause for destroying the environment and the robot. There are multiple ways of avoiding the mine exploding path. Since we have the navigation stack supporting the avoidance of the obstacles, the mine is updated into the Map Server as an obstacle and the mine is also avoided.

Chapter 4

Algorithm and Simulation results

The mobile robots with multi-sensor fusion has the capabilities of performing varied variety of tasks, drawn by the baseline of the sensors being used. This chapter focusses on the algorithms of finding mines in a minefield being an environment specific task of navigating around the field and detecting mines using a metal detector sensor. Mine detection in a given field can be explained as a phenomena of reading mine related signals and predicting the location. Since the mines are laid below the ground, the field of vision gets restricted to the metal detector location. Considering a stationary minefield region, this chapter considers the detection of mines over the metal detector region by localizing the mine signals and classifying from metal signals. The optimal detector region is controlled by factors like the non-holonomic vehicle constraints and the metal detector moving arm constraints.

In this chapter, mine localization using simple non-linear regression, least square method, unconstrained non-linear estimation and constrained non-linear estimation are discussed in the section 4.1. Followed by the support vector machine classification technique in section 4.2 to distinguish between different kind of signals (mines and metals). Section 4.3 deals with the strategy to avoid the mine region on localizing it in a minefield and navigate to be safe from the blast. Along with the description of the algorithms, it focusses on the simulation results. The proposed estimation algorithms are simulated on various Gaussian models and simulated models for estimating the mine center with its varying amplitude and variance parameters. MATLAB simulation results are described taking a differential drive robot into consideration with a moving arm to act as a metal detector to read the ground field environment signals. In this simulator, the

metal detector reads the signals at every position and calculates the detection alert for the algorithms to fall in place.

4.1 Field parameter estimation

The discussion of a mine or a metal signal can be considered to be a Gaussian distribution model depicting a maximum strength at the center with a reduction in strength as the metal detector moves away from the center. This section deals with the Gaussian field parameter estimation for proper localization.

4.1.1 Gaussian field parameter estimation using linear regression

Linear regression is a means to study the linear and additive relationship between the variables in estimating the dependent variable having known the other independent variables [27]. An estimation process is based on the collected data at the sampling locations. The sampling locations x, y which represents the position of the detector is given by

$$X = [x\ y] \tag{4.1}$$

With the general mine region represented by

$$F = a.g(X) \tag{4.2}$$

where the parameters a is linear and to be estimated root function of the region, $g(X)$ is a non-linear Gaussian identity function given by

$$g(X) = g(x, y) = \exp(-\left(\frac{(x - x_c)^2 + (y - y_c)^2}{2\sigma^2}\right)) \tag{4.3}$$

x_c & y_c are the known centers of the Gaussian with constant standard deviation σ .

Considering n samples at locations $X_1, X_2, \ldots, X_n$, the Gaussian mine region depends linearly on the coefficient a via position-dependent functions and can estimate

the linear unknown coefficient from linear regression method as described in [28] and [27].

$$\begin{aligned} F_1 &= a.\, g(X_1) \\ F_2 &= a.\, g(X_2) \\ &\vdots \\ F_n &= a.\, g(X_n) \end{aligned} \tag{4.4}$$

$$\tau = [a] = (g(X_i))^{+}{}_{i \le n} \begin{bmatrix} F_1 \\ \vdots \\ F_n \end{bmatrix} = M_n^{+} \begin{bmatrix} F_1 \\ \vdots \\ F_n \end{bmatrix}$$

Thus estimating the linear height parameter of the Gaussian distribution using the closed form pseudo inverse.

$$M_n^{+} = (M_n^T M_n)^{-1} M_n^T$$

$$\tau = \left(\sum_{i=i}^{n} \left(g(X_i) \right)^2 \right)^{-1} \sum_{i=i}^{n} F_i g(X_i) \tag{4.5}$$

4.1.1.1 Simulation result of parameterized Gaussian field

A 2D non-linear Gaussian model with a linear height is used as shown in Figure 4-6(a), with the desired Gaussian parameters as given below but keeping the variance constant with standard deviation $\boldsymbol{\sigma}$ = 1:

$$X = [x\ y\ a]$$

$$Actual\ parameters: X_{actual} = [5\ 5\ 1]$$

Figure 4-6(b) shows the top view of Gaussian field whose data at the sampled points marked in red is used to estimate the height of the Gaussian a. Using the least square estimation technique on the sampled data points, the Gaussian strength is

calculated and depicted in Figure 4-2 Height estimation of the Gaussian function where the other parameters like the centers and variance are known.

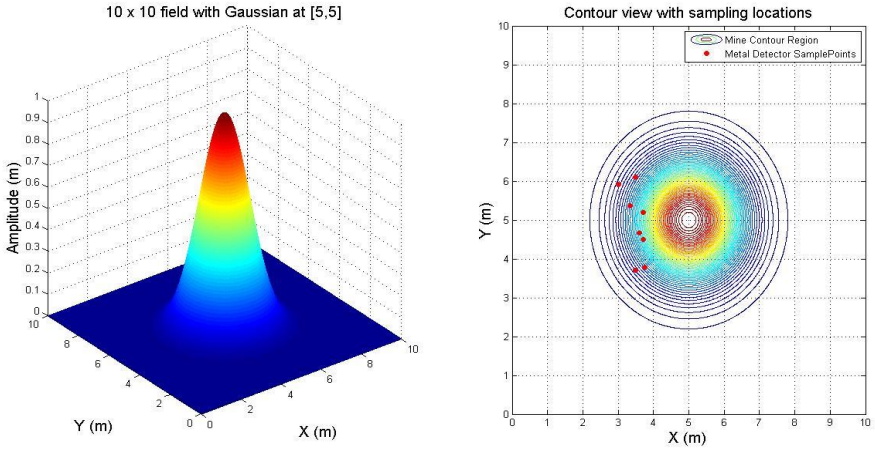

Figure 4-1 (a) 2-D Gaussian at [5, 5] (b) Contour view with sampling location

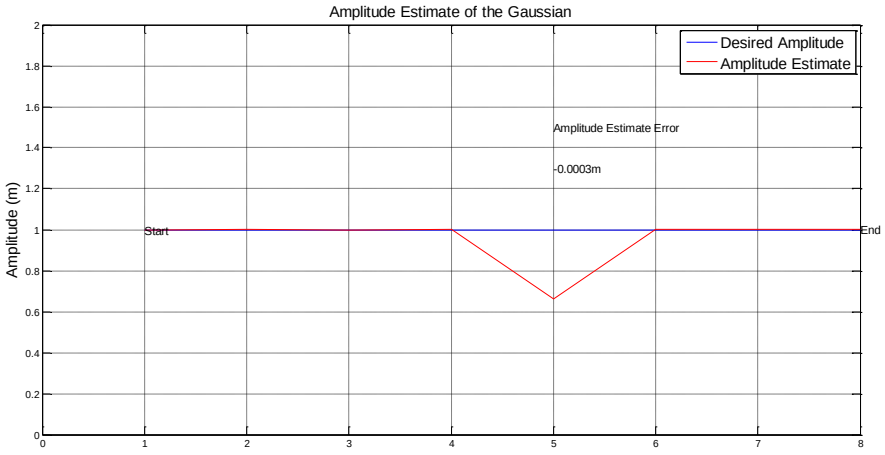

Figure 4-2 Height estimation of the Gaussian function

4.1.1.2 Simulation Result of simulated mine data from HRATC

In this case, the simulator mine data from the HRATC simulator is used for the estimation of the mine location and the highest value of the peak. As described about the

Vallon VMP3 metal detector, each coil has 3 independent channel data being published while scanning for metals or mines. Thus, Figure 4-9 is the left coil simulated data with having a center of the mine data sample at [5.55m, 2.85m].

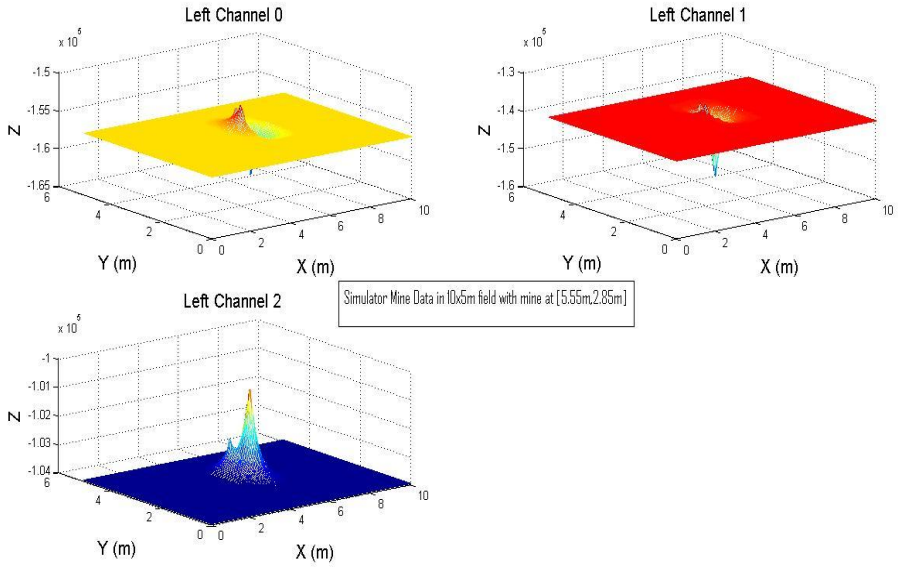

Figure 4-3 Left Coil Channel Data from HRATC Simulator

As described in section 3.1 about the detection alert of the pulse induction coils with respect to the coils, the detection alert for the left coil from the channel data is calculated using Equation 3.1 to obtain a resultant signal in Figure 4-9 (a) and (b) its contour plot with marked sampled locationsFigure 4-10. Hardware Framework with standard deviation $\boldsymbol{\sigma}$ = 0.14 on realizing the mine variance from the simulator, the maximum signal strength and location of the mine center are estimated using the below initial parameters:

$$X = [x\ y\ a]$$

$$Actual\ parameters: X_{actual} = [5.55\ 2.85\ 96520.0]$$

$$Guess\ parameters: X_{initial} = [5.2\ 2.6\ 80000]$$

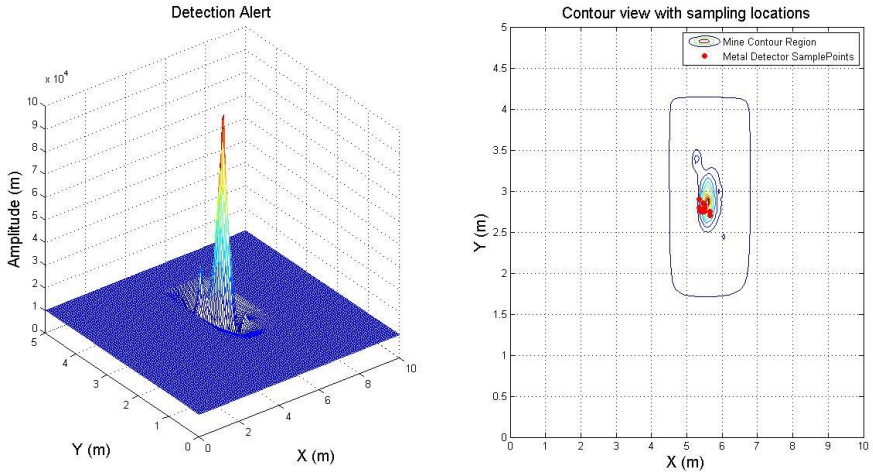

Figure 4-4 (a) Left Coil Detection Alert Signal across the minefield (b) Contour plot with sampled locations

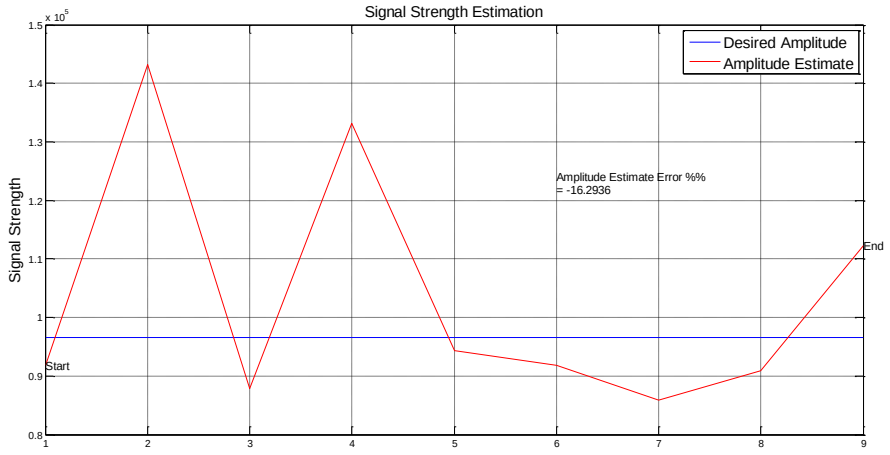

Figure 4-5 Mine strength estimation

On re-iterating with next estimated parameters for optimizing the Gaussian function to overlap the mine signal, the center location and the signal strength is estimated as shown in Figure 4-11 and Figure 4-12. This localization will help us avoid the mine region and getting the robot move at a safer distance from the mine. This

method is able to estimate the center as close with an error of 4cm on the simulated data but with poor coil signal strength estimation.

4.1.2 Gaussian Field parameter estimation using nonlinear Least-Square Minima

A Gaussian field is nonlinear in distribution and the linear regression does not satisfy in determination Gaussian centers without it being known. A non-linear least square fitting assume the function to be a known analytic form depending on n-parameters (λ) and considers the overdetermined set of m equations tabulated over m sample points given by $y_1 = f(x_1), \dots, y_m = f(x_m)$.

$$\begin{aligned} y_1 &= f(x_1; \lambda_1, \lambda_2, \dots, \lambda_n) \\ &\vdots \\ y_m &= f(x_m; \lambda_1, \lambda_2, \dots, \lambda_n) \end{aligned} \tag{4.6}$$

The goal is to solve these equations to obtain the values $\lambda_1, \lambda_2, \dots, \lambda_n$ which will satisfy the system of equations. Having an initial guess λ_i for the estimated parameters, we define

$$d\beta_i = y_i - f(x_i; \lambda_1, \lambda_2, \dots, \lambda_n) \tag{4.7}$$

The below equation provides a linearized estimate for the changes $\mathrm{d}\lambda_i$ needed to reduce $d\beta_i$ to 0;

$$d\beta_i = \sum_{j=1}^{n} \frac{\partial f}{\partial \lambda_j} d\lambda_j \Bigg|_{x_i \lambda} \tag{4.8}$$

For $i = 1, \dots, m$ where $\lambda \equiv (\lambda_1, \dots, \lambda_n)$ and can be written in component form as;

$$d\beta_i = A_{i\,j} d\lambda_j$$

$$A_{i\,j} = \begin{bmatrix} \frac{\partial f}{\partial \lambda_1}\Big|_{x_1 \lambda} & \cdots & \frac{\partial f}{\partial \lambda_n}\Big|_{x_1 \lambda} \\ \vdots & \ddots & \vdots \\ \frac{\partial f}{\partial \lambda_1}\Big|_{x_m \lambda} & \cdots & \frac{\partial f}{\partial \lambda_n}\Big|_{x_m \lambda} \end{bmatrix} \tag{4.9}$$

Defining a concise matrix form of $d\beta = A\, d\lambda$ where $d\beta$ is an m-vector and $d\lambda$ is an n-vector. Applying transpose of A, we get

$$A^T d\beta = (A^T A)\, d\lambda \tag{4.10}$$

Which can be solved for $d\lambda$ using standard matrix techniques and iteratively this offset is applied to λ and new $d\beta$ is calculated until the element $d\lambda$ becomes smaller. The convergence is often greatly improved with initial guess close to best-fit and hence an average in the sampled points is chosen. And after the final iteration, the sum of the square residuals is given by $R^2 = d\beta d\beta$

4.1.2.1 Simulation Result of 2D Gaussian function

A 2D non-linear Gaussian model is used as shown in Figure 4-6(a), with the desired Gaussian parameters as given below but keeping the variance constant with standard deviation $\boldsymbol{\sigma}$ = 1:

$$X = [x\ y\ a]$$

$$Actual\ parameters: X_{actual} = [5\ 5\ 1]$$

$$Guess\ parameters: X_{initial} = [4.6\ 5.4\ 0]$$

Figure 4-6(b) shows the top view of Gaussian field whose data at the sampled points marked in red is used to estimate the centers of the Gaussian along with the height of the non-linear function. Using the least square non-linear estimation technique on the sampled data points, the estimated center of the Gaussian after 28 iterations is [x, y] = [4.71m,4.91m] with an approximate error of 30 m if the field is considered to be 10m x 10m as shown in Figure 4-7 with the plot showing the estimated values at every iterations. Figure 4-8 results the estimated height on every iterations of the algorithm to

reach the desired amplitude of 1m of the Gaussian surface.

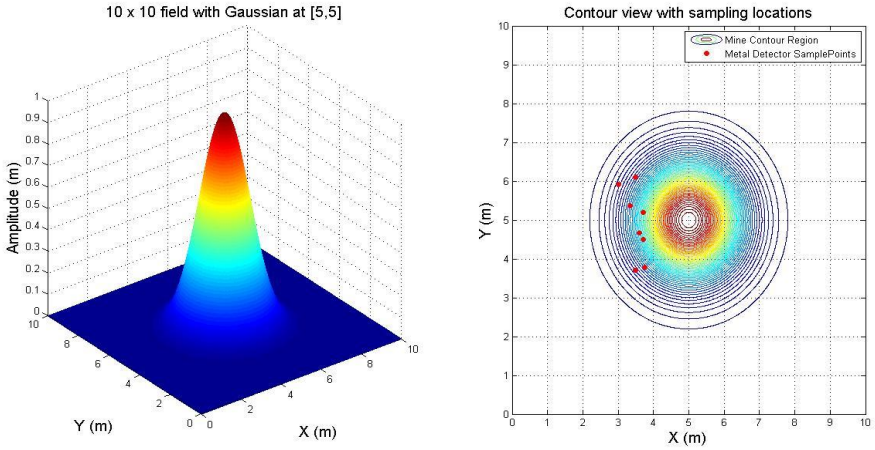

Figure 4-6 (a) 2-D Gaussian at [5, 5] (b) Contour view with sampling location

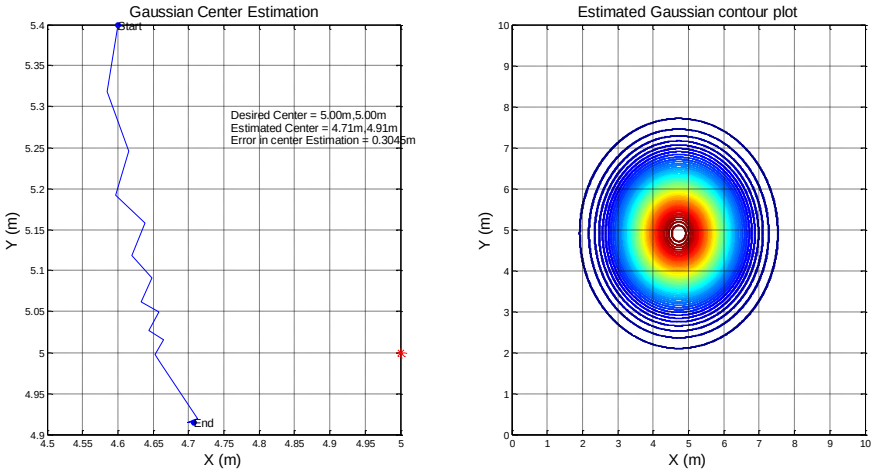

Figure 4-7 Gaussian center estimation along with its contour view

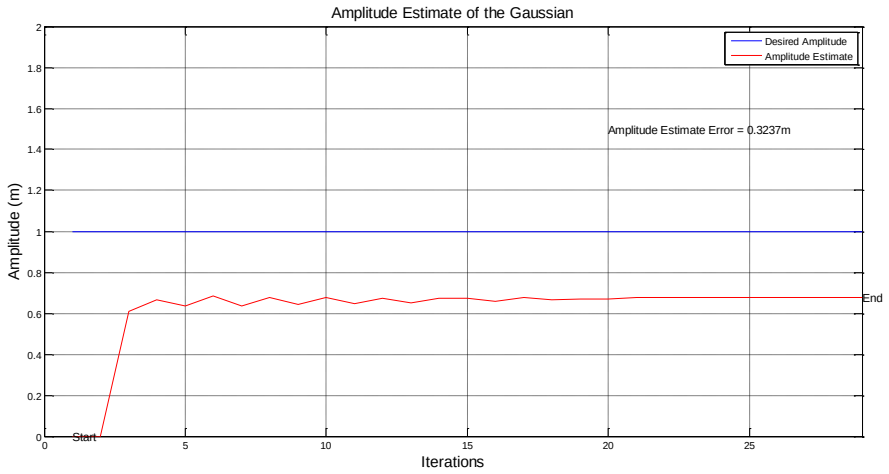

Figure 4-8 Height estimation of the Gaussian function

4.1.2.2 Simulation Result of simulated mine data from HRATC

In this case, the simulator mine data from the HRATC simulator is used for the estimation of the mine location and the highest value of the peak. As described about the Vallon VMP3 metal detector, each coil has 3 independent channel data being published while scanning for metals or mines. Thus, Figure 4-9 is the left coil simulated data with having a center of the mine data sample at [5.55m, 2.85m].

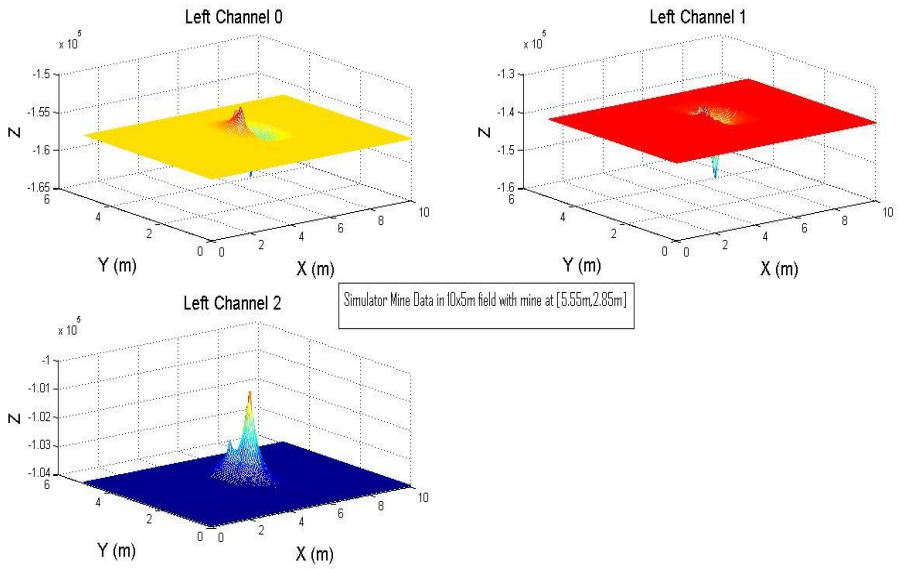

Figure 4-9 Left Coil Channel Data from HRATC Simulator

As described in section 3.1 about the detection alert of the pulse induction coils with respect to the coils, the detection alert for the left coil from the channel data is calculated using Equation 3.1 to obtain a resultant signal in Figure 4-9 (a) and (b) its contour plot with marked sampled locationsFigure 4-10. Hardware Framework with standard deviation $\boldsymbol{\sigma}$ = 0.14 on realizing the mine variance from the simulator, the maximum signal strength and location of the mine center are estimated using the below initial parameters:

$$X = [x\ y\ a]$$

$$Actual\ parameters: X_{actual} = [5.55\ 2.85\ 96520.0]$$

$$Guess\ parameters: X_{initial} = [5.2\ 2.6\ 80000]$$

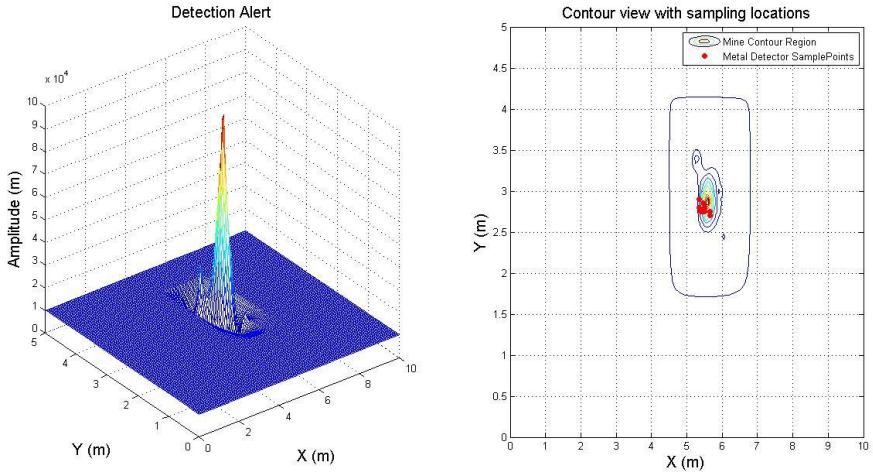

Figure 4-10 (a) Left Coil Detection Alert Signal across the minefield (b) Contour plot with sampled locations

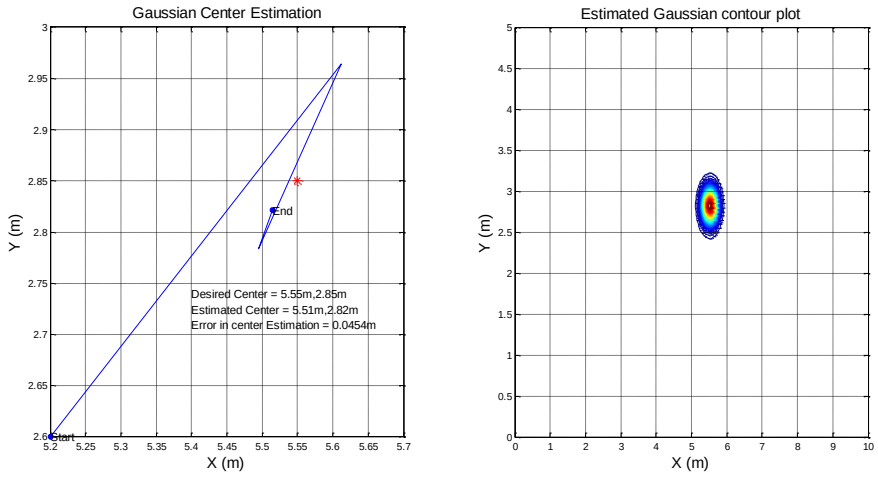

Figure 4-11 Mine location estimation using LSM non-linear optimization

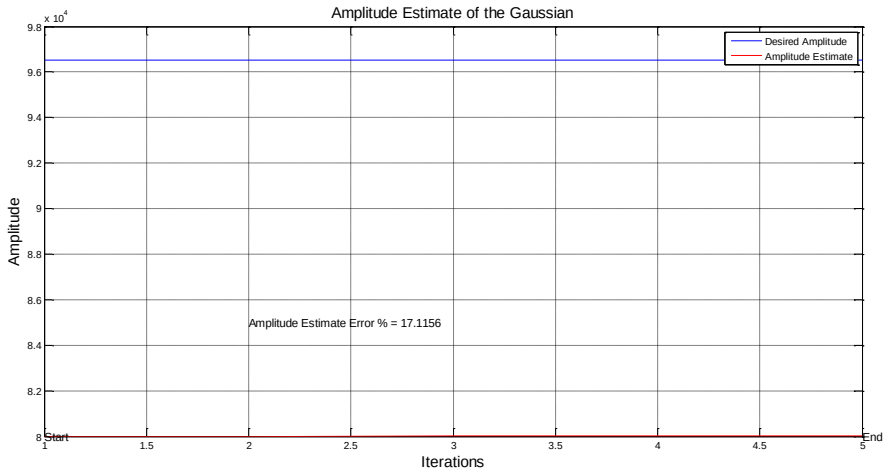

Figure 4-12 Mine strength estimation

On re-iterating with next estimated parameters for optimizing the Gaussian function to overlap the mine signal, the center location and the signal strength is estimated as shown in Figure 4-11 and Figure 4-12. This localization will help us avoid the mine region and getting the robot move at a safer distance from the mine. This method is able to estimate the center as close with an error of 4cm on the simulated data but with poor coil signal strength estimation.

4.1.3 Estimation using Unconstrained Non-Linear Optimization

The above model is a closed loop process and it is observed that the linear parameter a is not been attained. To estimate the linear parameter a and centers x_c & y_c of the non-linear Gaussian basis function, we try using the unconstrained optimization technique. The sampling locations [x, y], mine region and the basis function are represented as

$$X = [x\ y] \tag{4.11}$$

With the general mine region represented by

$$F = a.g(X) \tag{4.12}$$

where the parameters a is linear and the root function of the region, $g(X)$ is a non-linear Gaussian identity function given by

$$g(X) = g(x, y) = \exp(-\left(\frac{(x - x_c)^2 + (y - y_c)^2}{2\sigma^2}\right)) \tag{4.13}$$

The unconstrained minimization technique uses a 'quasi-newton' algorithm to evaluate the Gaussian function parameters. This method formulates a curvature information at each iteration to formulate a quadratic model problem. The method is iterative, generating a sequence of points x_k starting at initial point x_o and converging to an ideal x^*.

Considering n samples at locations $X_1, X_2, \dots, X_n$, the Gaussian mine region depends linearly on the coefficient a with respect to the non-linear centroid-dependent root function, we are trying to find the unknown variables a, x_c, y_c keeping the variance σ^2 constant. The estimated functions wrt to the estimated centers and amplitude is given by the below equations:

$$\begin{aligned} F_1 &= a * g(X_1) \\ F_2 &= a * g(X_2) \\ &\vdots \\ F_n &= a * g(X_n) \end{aligned} \tag{4.14}$$

Considering the equation (4.15) as the objective function is used to estimate the optimum values of a, x_c, y_c using the unconstrained non-linear optimization techniques.

$$min_X f(x) = \sum_{i=1}^{n} abs(y_i - F_i)) \tag{4.15}$$

4.1.3.1 Simulation Result of 2D Gaussian function

Similar to the experiment carried out on the earlier simulation using least square method non-linear optimization, the same model is considered with constant standard deviation $\boldsymbol{\sigma}$ = 1 and other parameters as follows:

$$X = [x\ y\ a]^T$$

$$Actual\ parameters: X_{actual} = [5\ 5\ 1]^T$$

$$Guess\ parameters: X_{initial} = [3.5125\ 4.9063\ 0.1]^T$$

Figure 4-13(b) shows the top view of Gaussian field whose data at the sampled points marked in red is used to estimate the centers of the Gaussian along with the height of the non-linear function. The initial guess of the mine center is obtained by the average of the sampled data points. Using the unconstrained non-linear optimization technique on the sampled data points, the estimated center of the Gaussian after 25 iterations is [x, y] = [4.99m,4.99m] with an approximate error of 0.1cm if the field is considered to be 10m x 10m as shown in Figure 4-79 with the plot showing the estimated values at every iterations. Figure 4-8 results the estimated height on every iterations of the algorithm which is converging to the desired height of the Gaussian's data being used for the simulation.

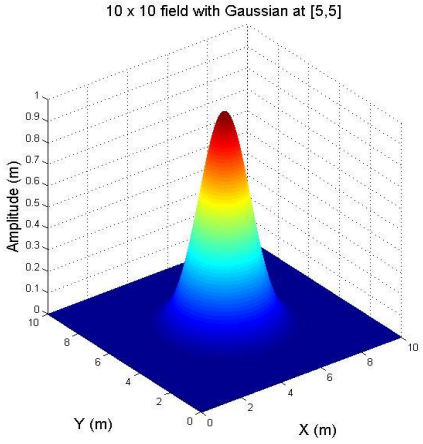

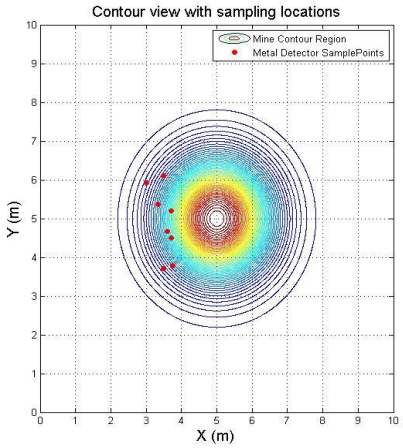

Figure 4-13 (a) 2-D Gaussian at [5, 5] (b) Contour view with sampling location

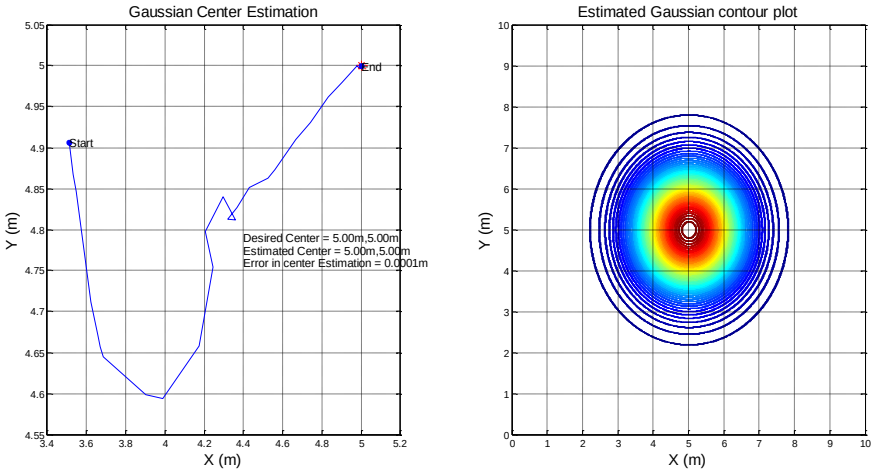

Figure 4-14 Gaussian center estimation along with its contour view

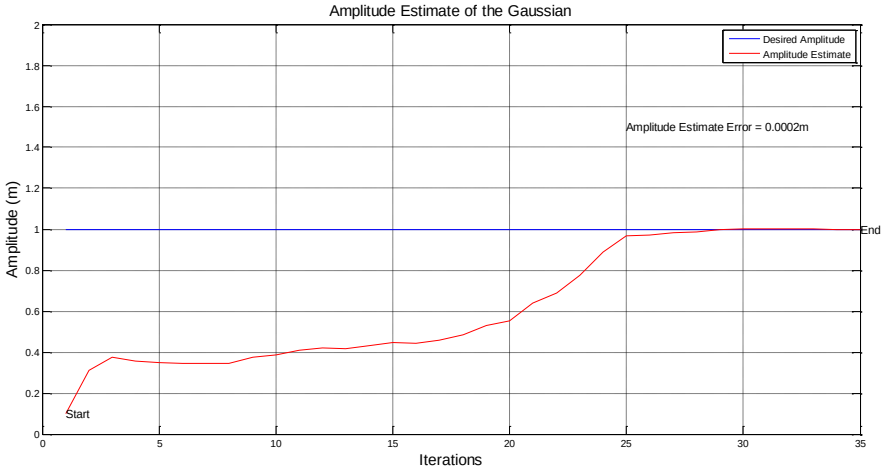

Figure 4-15 Height estimation of the Gaussian function

4.1.3.2 Simulation Result of simulated mine data from HRATC

This is a similar simulation carried out with the left coil data as described in section 4.1.2.2. The metal detector reading over the minefield is simulated as in Figure

4-9 placing a mine at [5.55m, 2.85m] generating a mine region with a variance of 0.0196m^2 once the detection alert is calculated using the Vallon VMP3 detection calculator shown in Figure 4-16(a).

With the sampled data points being collected (assuming the robot has swept over the mine region) shown in the Figure 4-16(b) the optimization is carried out using the unconstrained non-linear optimization to achieve the desired mine region parameters with an initial guess to be the average of the location of the sampled points.

$$X = [x\ y\ a]^T$$

$$Actual\ parameters: X_{actual} = [5.55\ 2.85\ 96520.0]^T$$

$$Guess\ parameters: X_{initial} = [5.4778\ 2.7833\ 0.1]^T$$

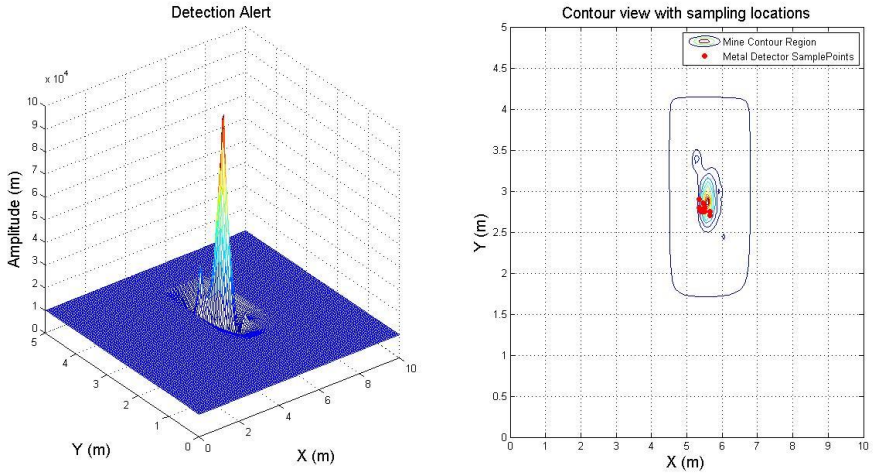

Figure 4-16 (a) Left Coil Detection Alert Signal across the minefield (b) Contour plot with sampled locations

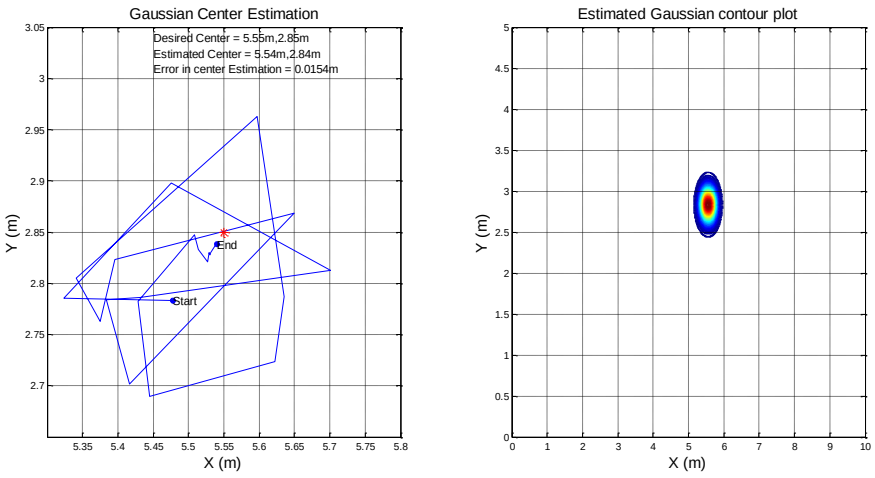

Figure 4-17 Mine location estimation using LSM non-linear optimization

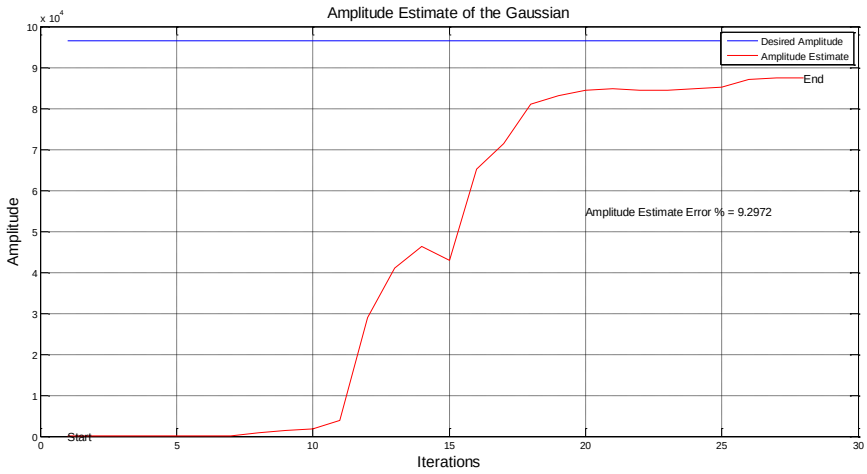

Figure 4-18 Mine strength estimation

The results of the mine center location and the mine strength prediction converges to the desired values with an approximate 30 iterations. It is observed the center estimation error is 1.5cm and the amplitude % = 9% giving a better performance than the least square optimization technique.

4.1.4 Estimation using Constrained Non-Linear Optimization

With the estimation of the amplitude and the position shifting parameters of the Gaussian mine region, based on the mines depth, the width of the region also vary. In the above unconstrained optimization the variance was kept constant. The constrained optimization technique uses 'Interior-Point' algorithm for optimizing non-linear equations with constrained and bounded parameters. Here with bounded parameters and no initial guesses with the amplitude and the parameter, this technique estimates all the unknown parameters namely the amplitude a, centers x_c & y_c and the width of the Gaussian $\boldsymbol{\sigma}$. The sampling locations, field region model and the Gaussian function are again represented by the above equations (4.11), (4.12), (4.13)

The constrained non-linear optimizer minimizes the function f(x) focused on linear/non-linear equality and inequality constraints and the bounded region specified by

$$lb \leq x \leq ub$$
$$where\ x = [x\ y\ a]^T \tag{4.16}$$

The measured values $z_i; i = 1\ to\ n$ along the sampling locations X_i, we use the following objective function for optimizing the coefficients specified in equation (4.16) with constant standard deviation $\boldsymbol{\sigma}$.

$$min_x f(x) = \sum_{i=1}^{n} |z_i - x(3).e^{-\frac{(x_i - \ x(1))^2 + (y_i - x(2))^2}{2\sigma^2}}| \tag{4.17}$$

4.1.4.1 Simulation Result of 2D Gaussian function

The simulation method described in section 4.1.3.1 is carried out with the exact same conditions. The Figure 4-20 Gaussian center estimation along with its contour view and Figure 4-21 Height estimation of the Gaussian function describes the outcome of the optimizer with the following parameters defined along with a constant $\boldsymbol{\sigma}$ = 1.

$$X = [x\ y\ a]^T$$
$$Actual\ parameters: X_{actual} = [5\ 5\ 1]^T$$

$$Guess\ parameters: X_{initial} = [3.5125\ 4.9063\ 0.1]^T$$

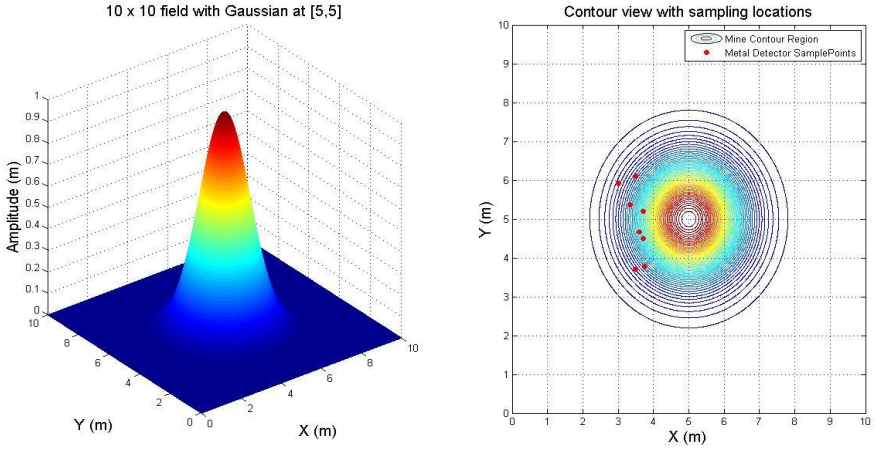

Figure 4-19 (a) 2-D Gaussian at [5, 5] (b) Contour view with sampling location

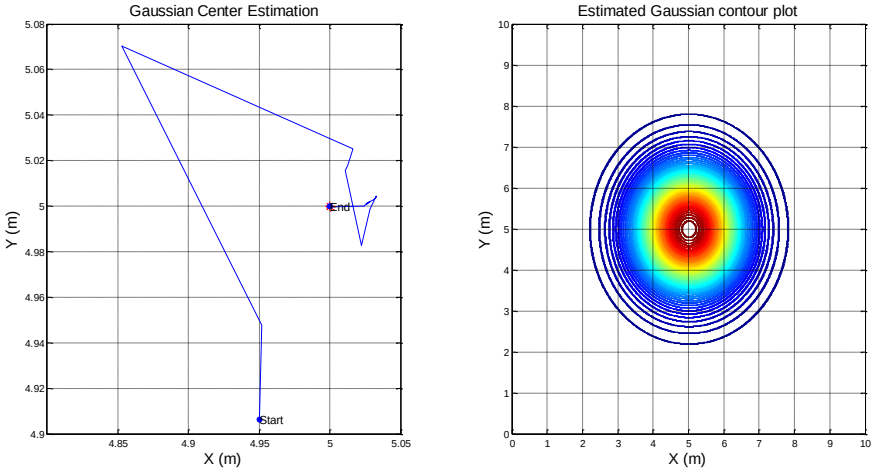

Figure 4-20 Gaussian center estimation along with its contour view

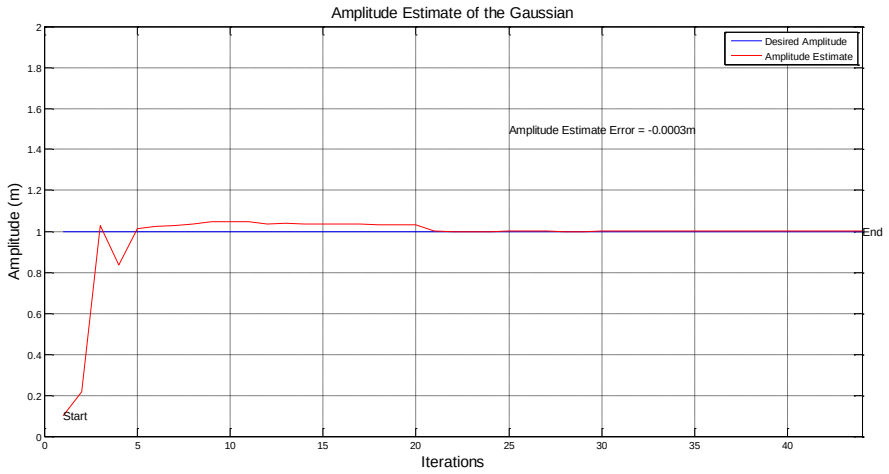

Figure 4-21 Height estimation of the Gaussian function

4.1.4.2 Simulation Result of simulated mine data from HRATC

Similarly the section 4.1.3.2 procedure is followed to achieve the outcome of the constrained non-linear optimizer considering the parameters depicted as below and Figure 4-9 & Figure 4-22.

$$X = [x\ y\ a]^T$$

$$Actual\ parameters: X_{actual} = [5.55\ 2.85\ 96520.0]^T$$

$$Guess\ parameters: X_{initial} = [5.4778\ 2.7833\ 0.1]^T$$

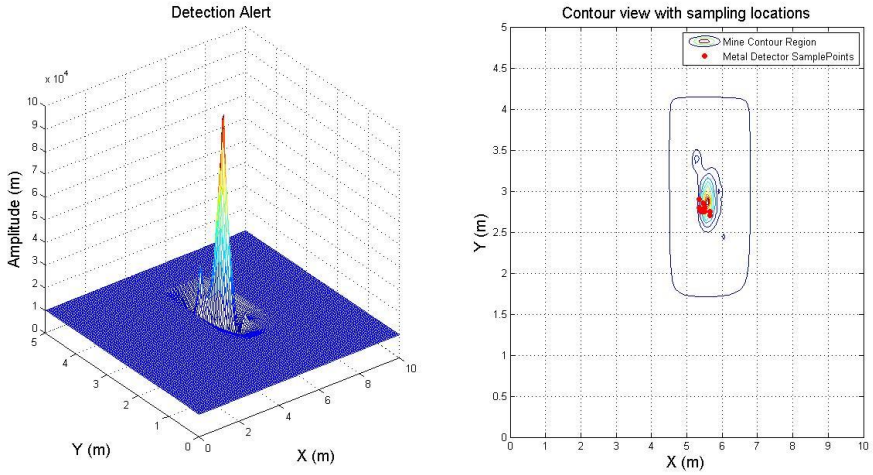

Figure 4-22 (a) Left Coil Detection Alert Signal across the minefield (b) Contour plot with sampled locations

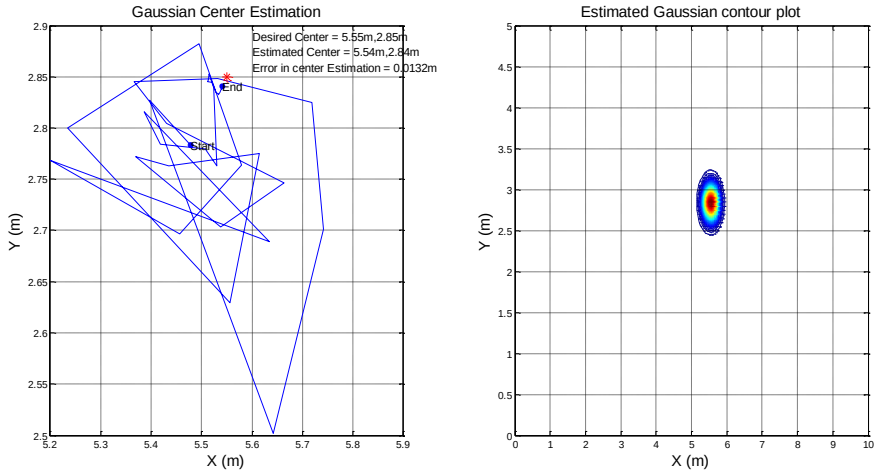

Figure 4-23 Mine location estimation using LSM non-linear optimization

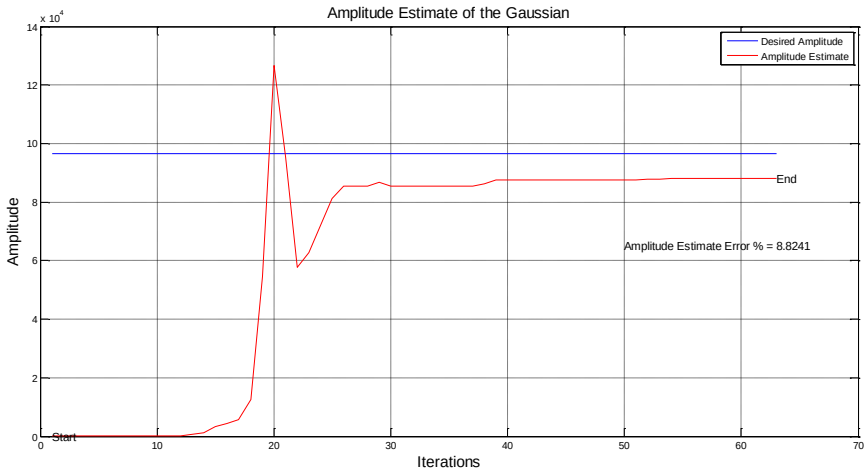

Figure 4-24 Mine strength estimation

The constrained algorithm has boundary conditions on the estimating parameters which helps the predictions to be bounded. Hence the error in estimating the Gaussian parameters (mine data readings showing the similar properties of the Gaussian) is small considering the above theories and hence a bounded non-linear estimation algorithm was implemented in ROS C++ for working on Gazebo simulator and its theory is discussed in the next section.

4.1.5 Bound Constrained Optimization without derivatives

BOBYQA (Bounded Optimization by Quadratic Approximation) is an iterative algorithm by M.J.D Powell for finding minimum of a function F(x), in the absence of derivative information [29]. It is implemented in ROS C++ with the help of the NLOPT (non-linear optimization) library. It is free of gradient and hence the Gaussian function is minimized optimizing the unknown coefficients which is incorporated by applying a trust region method that forms quadratic models by interpolation. The unknown variables (components of x) are bounded by upper and lower limits. This technique was incorporated in ROS for the actual testing on the gazebo simulator for mine localization

since the constrained non-linear optimization using interior-point algorithm used by fmincon in MATLAB proved to be the best approach in estimating the mine center and the signal strength. On implementing this technique gives a similar result to the one discussed in sections 4.1.4.1 & 4.1.4.2.

4.2 Support Vector Machine (SVM) Classifier

Support vector machines are supervised learning models that analyze data and recognize patterns for classification with associated learning algorithms. As discussed in [30], the SVM classifier is used for multiple reasons involving continued process even with many local minima in the given model. Also its independent ability towards the complexity of the learning algorithm helps classification easy. SVM put forth an algorithm to maximize the separating margin between the two classes, given by n data sets:$(x_i, d_i)|_{i=1:n}$; x_i representing the input vectors and d_i referring the class.
Training Data is given as input vectors x and class d which is referred as metal or mine.

$$\{x_i, d_i\}; i = 1,2,3, \dots, n \tag{4.18}$$

The linear separable hyper-plane is given by:

$$g(x) = w^T x + b = 0; w = weights\ and\ b = biases \tag{4.19}$$

Hyper-plane is considered optimal when separating the margin between classes, achieved by computing

$$\min_w 0.5 w^T w$$
$$d_i(w^T x_i + b) \geq 1 \tag{4.20}$$

Leads to a minimization of a Lagrange function

(4.21)

$$J(w, b, \alpha) = 0.5w^T w \; - \; \sum_{i=1}^{n} \alpha_i [\, d_i(w^T x_i + b) - 1]$$

Where α being a non-zero Lagrange coefficient [30].

SVM can implement different activation functions namely: linear, polynomial, radial or sigmoid. If we required a capability of threshold, then the linear classifier would have sufficed. But in this case, we are figuring a way to classify between metals having different signature values. The mine related metals have a least signature values and sometimes still coincide with the metal signature values. So to achieve a better distinguishing between metals and surrogate mines (simulated data set), we use the Radial Basis Function (RBF). It uses a Gaussian function to find the decision manifold for enclosing the boundaries between multiple class.

$$f(x) = \; \beta \exp(-\sum_{i} \left[\frac{(x_i - c_i)}{\sigma_i}\right]^2) \qquad (4.22)$$

Where the centroid c_i , constants β and σ are dependent on the training data x_i.

The below figures depicts all channels data for mine and metal used for training the SVM Classifier for individual coils. Here the training data sets are the three channel raw data from each individual coil and the class is either a ‘mine’ or a ‘metal’ which can be considered as ‘+1’ or ‘-1’ respectively. In which case, on classification outcome, the positive values will be more prone to being a mine than a metal. The RBF neural network forms a hidden layer with a centroid c_i and a smoothing factor σ_i, which is involved in measuring the distance between the inputs (i.e classification data set). And thus the outcome is the highest if it is closest to the c_i suggesting a positive value for 1 class and –ve for the other. Mapping function similar to the Gaussian function are used in the RBF networks having the form of (4.22).

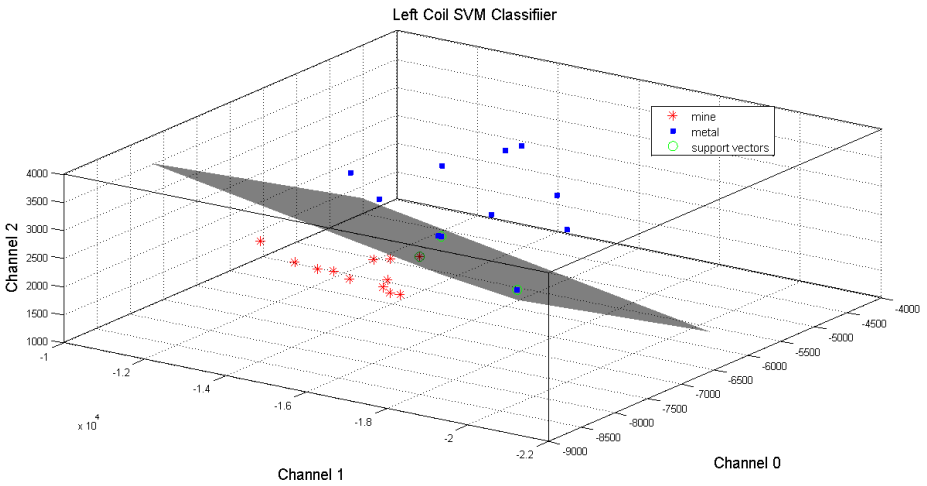

Figure 4-25 SVM classifier for Left coil using individual channel data

Table 4-1 Training Data for Classificaiton using Left Coil Metal Detector Channel readings with its classified result

Training Data for Left Coil Classifier				**Outcome Type**
Channel 0	Channel 1	Channel 2	Class	
-8314	-16940	2552	'mine'	**'mine'**
-6771	-12040	1583	'mine'	**'mine'**
-7971	-16200	2366	'mine'	**'mine'**
-8575	-17620	2752	'mine'	**'mine'**
-7231	-13760	1916	'mine'	**'mine'**
-7748	-15010	2227	'mine'	**'mine'**
-7232	-15170	2346	'mine'	**'mine'**
-7144	-13220	1830	'mine'	**'mine'**
-6095	-10080	1327	'mine'	**'mine'**
-7147	-15750	2422	'mine'	**'mine'**
-7721	-15902	2320	'mine'	**'mine'**
-6931	-14255	2041	'mine'	**'mine'**
-8974	-21175	3561	'metal'	**'metal'**
-6368	-17859	3425	'metal'	**'metal'**
-4570	-13619	2676	'metal'	**'metal'**
-4878	-14527	3052	'metal'	**'metal'**
-7123	-16170	2838	'metal'	**'metal'**
-5522	-11360	2442	'metal'	**'metal'**
-5386	-11840	1973	'metal'	**'metal'**
-6515	-15240	2382	'metal'	**'metal'**
-6184	-15930	2706	'metal'	**'metal'**
-7194	-19470	3469	'metal'	**'metal'**
-4377	-11740	2033	'metal'	**'metal'**

The Figure 4-25 shows the SVM classification decision manifold corresponding to the data sets mentioned in Table 4-1 for the left coil. The data sets are the raw channel data of the individual coil namely Channel 0, Channel 1 and Channel 2 with a class specified as ‘mine’ (+1) and ‘metal’ (-1). Due to a radial basis function, the decision boundary has enclosed the data set which helps better classification as seen in the other coil classification (Figure 4-26 & Figure 4-27).

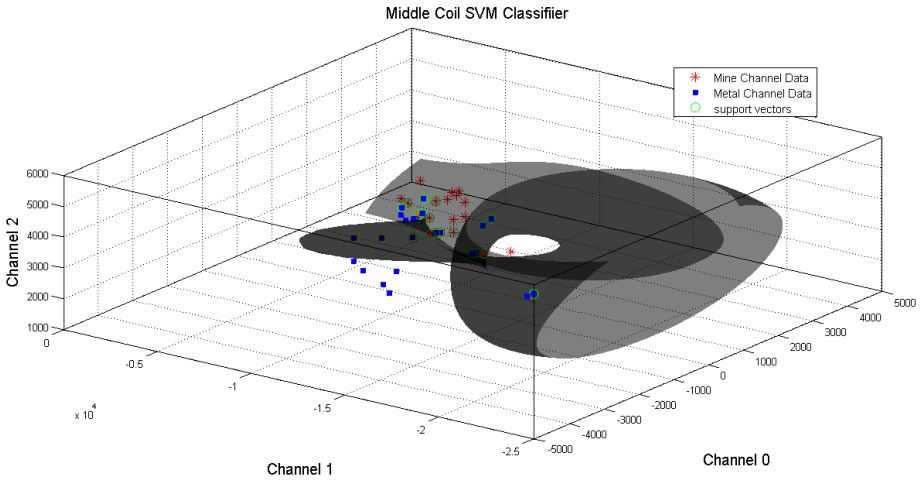

Figure 4-26 SVM classifier for Middle coil using individual channel data

Table 4-2 Training Data for Classificaiton using Middle Coil Metal Detector Channel readings with its classified result

Training Data for Left Coil Classifier				**Outcome Type**
Channel 0	Channel 1	Channel 2	Class	
1425	-9440	2930	mine'	**'mine'**
2641	-5634	2308	'mine'	**'mine'**
2432	-7572	2649	'mine'	**'mine'**
1404	-7590	2633	'mine'	**'mine'**
1278	-9094	2846	'mine'	**'mine'**
-1173	-16700	4066	'mine'	**'mine'**

Table 4.2—*Continued*

1904	-6136	2296	'mine'	**'metal'**
-1370	-15600	3947	'mine'	**'mine'**
2743	-6071	2368	'mine'	**'mine'**
2987	-3507	1786	'mine'	**'mine'**
3014	-6075	2388	'mine'	**'mine'**
3235	-5779	2383	'mine'	**'mine'**
4259	-1844	1666	'mine'	**'mine'**
3407	-2381	1554	'mine'	**'mine'**
275	-9735	2950	'mine'	**'mine'**
3151	-5570	2340	'mine'	**'mine'**
360	-10800	3120	'mine'	**'mine'**
1802	-6218	2230	'metal'	**'metal'**
574	-9693	2862	'metal'	**'mine'**
-1175	-14890	3780	'metal'	**'metal'**
-4184	-23470	5096	'metal'	**'metal'**
836	-11920	3487	'metal'	**'metal'**
2663	-4960	2288	'metal'	**'metal'**
1403	-7216	2733	'metal'	**'metal'**
1051	-6990	2641	'metal'	**'metal'**
1883	-5179	2153	'metal'	**'metal'**
2715	-3712	1794	'metal'	**'metal'**
1726	-6151	2239	'metal'	**'metal'**
416	-9722	2921	'metal'	**'mine'**
-1546	-15320	3999	'metal'	**'metal'**
-4809	-24280	5452	'metal'	**'metal'**
313	-12450	3597	'metal'	**'metal'**
1474	-3441	1368	'metal'	**'metal'**
1023	-5752	1910	'metal'	**'metal'**
514	-8364	2537	'metal'	**'metal'**
111	-5949	1615	'metal'	**'metal'**
-523		1852	'metal'	**'metal'**
-1497	-10520	2290	'metal'	**'metal'**
-1929	-11630	2366	'metal'	**'metal'**
-1094	-10470	2498	'metal'	**'metal'**

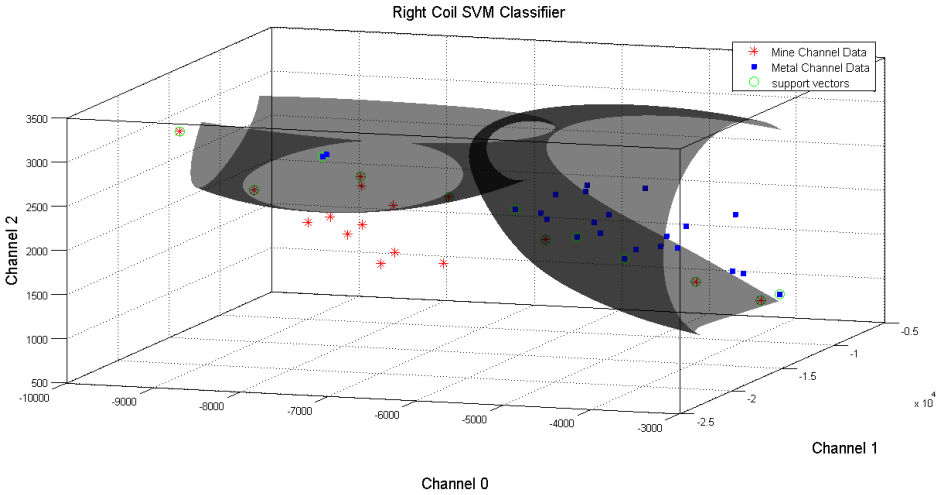

Figure 4-27 SVM classifier for Right coil using individual channel data

Table 4-3 Training Data for Classificaiton using Middle Coil Metal Detector Channel readings with its classified result

Training Data for Left Coil Classifier				**Outcome Type**
Channel 0	Channel 1	Channel 2	Class	
-8768	-17260	2348	'mine'	**'mine'**
-7883	-14240	1843	'mine'	**'mine'**
-8101	-15520	1990	'mine'	**'mine'**
-7518	-14340	2084	'mine'	**'mine'**
-6806	-14990	2250	'mine'	**'mine'**
-9086	-21777	3231	'mine'	**'mine'**
-6102	-11620	1627	'mine'	**'mine'**
-8390	-15220	1895	'mine'	**'mine'**
-4748	-8517	1057	'mine'	**'mine'**
-8025	-14480	1743	'mine'	**'mine'**
-7627	-13250	1494	'mine'	**'mine'**
-7233	-11890	1320	'mine'	**'mine'**
-4169	-7138	804.59998	'mine'	**'mine'**
-7748	-15490	2357	'mine'	**'mine'**
-7827	-12920	1336	'mine'	**'mine'**
-7660	-16320	2508	'mine'	**'mine'**
-5470	-11630	1733	'metal'	**'metal'**
-4727	-10460	1541	'metal'	**'metal'**
-5946	-13420	2033	'metal'	**'metal'**
-7884	-17750	2822	'metal'	**'metal'**

Table 4.3—*Continued*

-5455	-12380	1894	'metal'	**'metal'**
-5282	-10900	1417	'metal'	**'metal'**
-5764	-11450	1666	'metal'	**'metal'**
-5225	-10280	1488	'metal'	**'metal'**
-4333	-8482	1193	'metal'	**'metal'**
-3936	-7297	892.5	'metal'	**'metal'**
-4201	-8530	1176	'metal'	**'metal'**
-4914	-10520	1550	'metal'	**'metal'**
-6216	-13600	2065	'metal'	**'metal'**
-7919	-17820	2797	'metal'	**'metal'**
-5937	-12890	1935	'metal'	**'metal'**
-4720	-11630	1738	'metal'	**'metal'**
-5658	-14430	2304	'metal'	**'metal'**
-5368	-13970	2334	'metal'	**'metal'**
-5318	-14260	2420	'metal'	**'metal'**
-3984	-11210	1995	'metal'	**'metal'**
-5203	-13140	2034	'metal'	**'metal'**
-4767	-13280	2361	'metal'	**'metal'**
-4516	-11440	1848	'metal'	**'metal'**

4.3 Potential Field Navigation with Obstacle and Mine Avoidance

The estimated mine location with its Gaussian intensity can be used as a repulsive potentials to keep the mine detector robots away from the mines. Similarly an attractive potential is given by the target or the goal points. This scalar potential field provides a vector field of conservative forces on its negative gradient which helps generating a navigational path. At a given point of the robot $X = [x, y]^T$, the net forces acting on the robot is the result of the target forces and the mine or obstacle forces which governs the robot to move to its next location. The below equations summarizes the path planning for collision-free navigation using the potential fields [31] [32].

$$\vec{F}(X) = \vec{F}_{goal}(X) + \sum_{i=1}^{n} \vec{F}_{obs_i}(X) = -\vec{\nabla}U(X) \tag{4.23}$$

Each forces defined in the eq (4.16) have their x and y components considering a 2D dimensional space for the mobile ground robots. Hence the force gradient is given by:

$$\vec{\nabla}U(X) = [\frac{\partial U}{\partial x}\ \frac{\partial U}{\partial y}]^T = [F_x\ F_y]^T \tag{4.24}$$

The following forces are considered in the potential field:

- Attractive forces:

$$Attractive\ potential: U_{att}(X) = k.\left[\left(x - x_{goal}\right)^2 + \left(y - y_{goal}\right)^2\right]^{0.5}$$

$$r = [\left(x - x_{goal}\right)^2 + (y - y_{goal})^2]^{0.5} \tag{4.25}$$

$$Attractive\ force: \vec{F}_{goal}(X) = -\vec{\nabla}U_{att}(X) = k.\frac{(X_{goal} - X)}{r}$$

- Repulsive forces from mines which are considered as obstacles:

$$Repulsive\ potential: U_{obs_i}(X) = \frac{k}{\left[\left(x - x_{obs_i}\right)^2 + \left(y - y_{obs_i}\right)^2\right]^{0.5}}$$

$$r_i = [\left(x - x_{obs_i}\right)^2 + (y - y_{obs_i})^2]^{0.5} \tag{4.26}$$

$$\vec{F}_{obs_i}(X) = -\vec{\nabla}U_{obs_i}(X) = \begin{cases} -\frac{k}{{r_i}^2}.\frac{\left(X_{obs_i} - X\right)}{r_i}; if\ r_i < r_0 \\ 0\ ; if\ \ r_i > r_0 \end{cases}$$

where k is the potential scaling factor and r_0 being the detection vicinity of the obstacle. This acting forces on the robot gives a trajectory to navigate through the minefield and avoid on its detection.

4.3.1 Trajectory planning simulation results using Potential Fields

As discussed above on the potential field generation once the mine is detected, here we show the simulation results using the forces on the goal points and the mines. In the Figure 4-28, the simulation of the robot is carried out. The robot is attached with an end-effector for visualization of a metal detector like situation which records its position and reads the field data which consists of the mine regions. Here the contour plots describe the metal regions with mine related signals highlighted. The end-effector acts like a metal detector which keeps sweeping the arena and if its locations reading go above the threshold level, then the data is recorded for its analysis. Once the sufficient data above the threshold is obtained, then the mine location is estimated using the non-linear optimization technique discussed in the section 4.1.4 followed by its classification as a mine or metal. Having the localization of the mine with respect to the robot field frame, the mine is considered to be an obstacle by adding its location onto the obstacle map. Due to this, a repulsive field is created around the mine forcing the robot to move away from the mine only if it is in close proximity. Or else this can force the robot to take unnecessary paths increasing the cost of movement even if the force is small coming from the mine. The path of the robot is traced depicting the robots avoidance to the mines and obstacles following a raster scan pattern for area coverage.

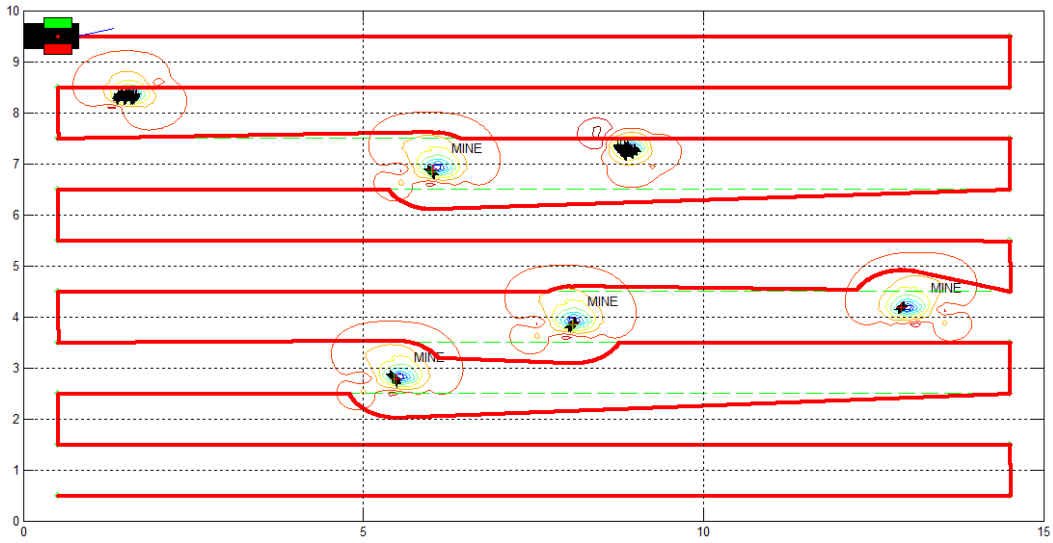

Figure 4-28 Raster scanning with mine avoidance using Potential field path Planning

4.4 Gazebo Simulation Results

The gazebo simulator is used to have the algorithm tested in the real scenario setup. Gazebo is well equipped with the libraries for the sensors like laser scanner, cameras, IMU, GPS and many more, which help implement an test the algorithms on the minefield. The HRATC also provided with a metal detector simulator with a PID controller for its arm sweep which acts similar to the real world capturing data on sweeping and publishing to the ROS node. This kind of setup helped the testing of the code mentioned in section 3.3 code framework for mine detection, mapping and avoidance. Due to the use of the classification technique, we have the mines on the simulator framework correctly distinguishable as seen in below figures. The Figure 4-29 shows a minefield with 4 mine related signals and 2 different kind of metal samples placed randomly. This is only the left detection alert value shown of the minefield. But the minefield can give out 9 channel data in total considering 3 coils and each coils with 3 channels individually with left coil 3 channel data shown in Figure 4-30

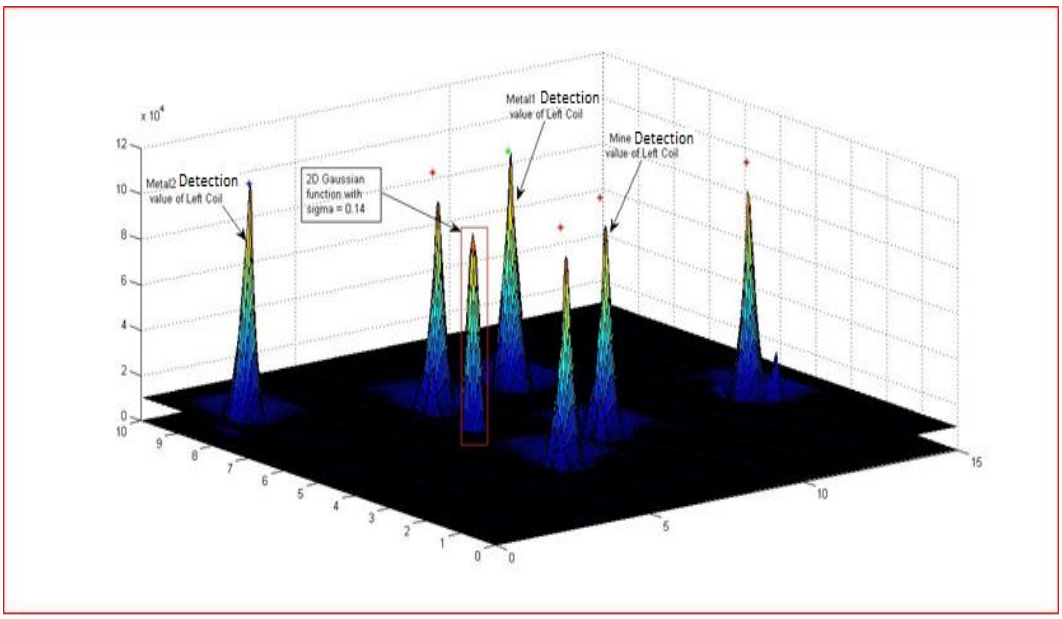

Figure 4-29 Left coil detection alert in the minefield

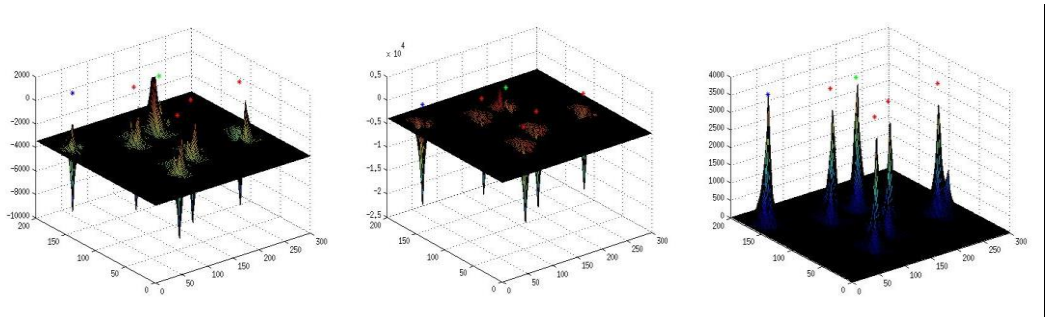

Figure 4-30 Left coil (a) channel0 (b) channel1 (c) channel2 signal in the minefield

Thus using these data for analysis purpose, the classifier and mine center estimation logic were implemented and proposed the solution for the given problem. The Figure 4-31 provides a gazebo simulator result. For the gazebo simulator, the minefield consisted of 5 mines in total and 7 metal pieces (of two types) randomly placed in the minefield. It is observed that on all three scenarios, none of the signals related to the metals were detected and only the mines were detected. The navigation stack of ROS

was used for avoiding the mines in which the mines were updated on the map server as an obstacle having a repulsive potential around it since the navigation stack uses the potential field technique to have an inflation radius around the obstacle. The flex planner takes the mobile platform into account and lays a spiral navigation waypoints for the robot to move around the minefield.

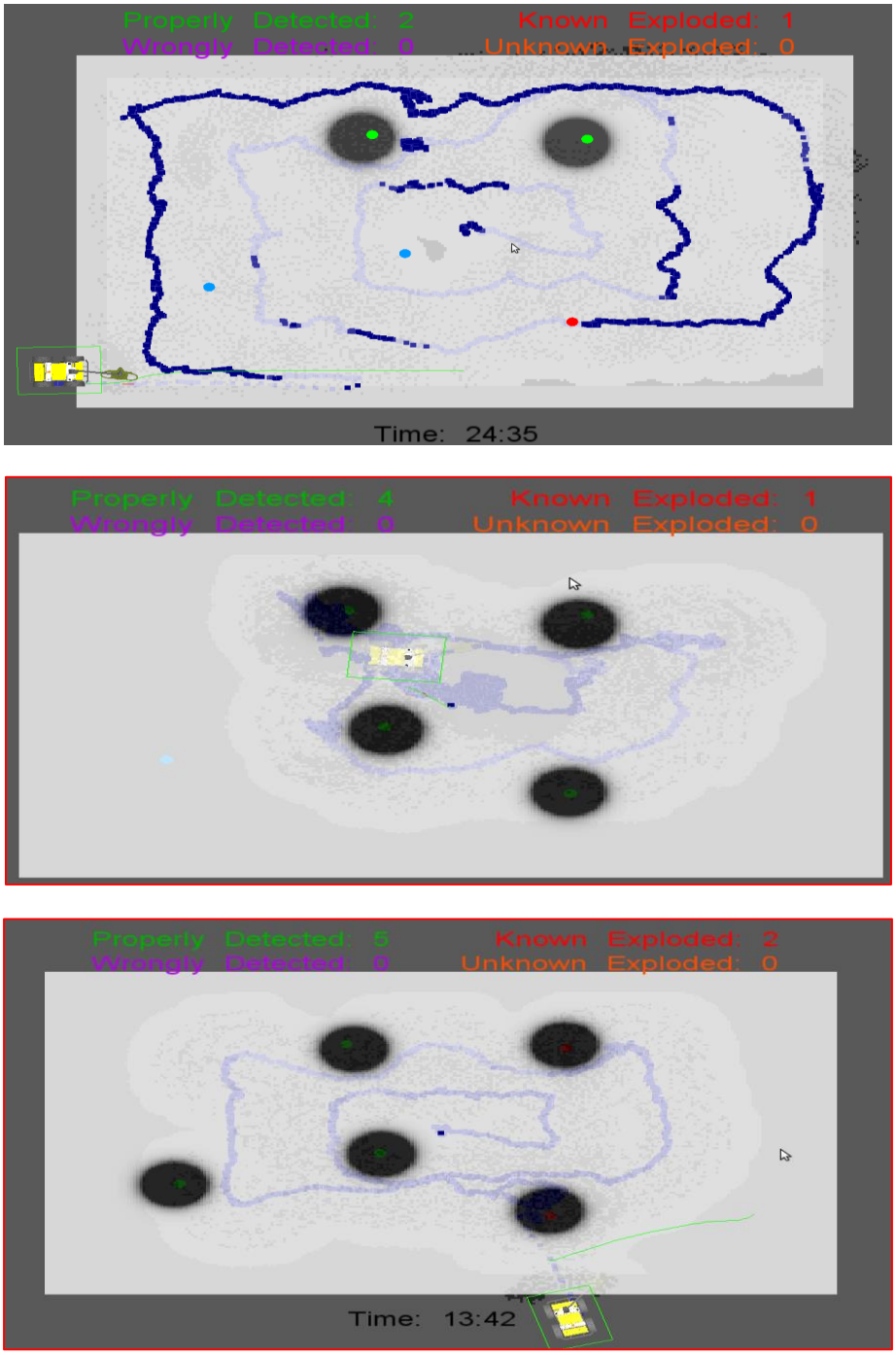

Figure 4-31 Gazebo Simulation Results

Chapter 5

Experimental Results

5.1 Neptune Infrastructure

The HRATC project is a simulation and a hardware testing challenge. However, the hardware testing was remotely done in Portugal and the challengers didn't have any freedom of testing it. Neptune is a Next Generation System (NGS) Lab robot based on LABO-3. It is a ground vehicle robot which is used as a testing platform for the HRATC project in our lab. LABO-3 robot from AAI Canada, Inc [19] is a small-size high payload autonomous platform for indoor use. For research purpose, it is equipped with a PC/104 processor from Advanced Digital Logic, Inc [33] for onboard processing.

The Neptune robot is a two –wheeled differential drive robot with virtually zero turning radius as shown in Figure 5-1 Neptune mobile robot with Laser, Camera and IMU and this chapter deals with the upgrades done on the platform for testing the mapping and autonomous navigation of avoiding obstacles. Its body is made of T6 60/61 aluminum and frame of stainless steel for its ruggedness and is designed with a flat top to which users may attach equipment of their own for research purposes. The top panel is made of aluminum with a thickness of 3.2 mm which can take a maximum payload of 28 kg.

Figure 5-1 Neptune mobile robot with Laser, Camera and IMU

Table 5-1 The hardware characteristics of LABO-3 robot [34]

Size	Length: 508 mm Width: 330 mm Height: 229 mm
Weight	25 kg
Max Payload	28 kg
Max Speed	1.8 m/s
Run Time	6 hours (with zero payload)
Battery	Sealed lead-acid battery (2 x 12V 21Ah) (Current rating may vary from 17Ah to 21Ah)
Motor Output	140W (x2)
Standard Processor	Digital Logic PC/104 processor
Basic Sensors	IR sensors Touch detection sensor within the bumpers.

The computer is located under the control panel at the rear of the body. This processor communicates with the I/O board through the address/data bus which acts as a controller which interfaces the LCD display, the switches and the external bus on the

control panel, the motor controller, IR sensors, and the touch sensors used in the bumpers.

Neptune runs on Intel® Pentium® M 1.8GHz processor and supports a 400MHz FSB with integrated Intel Graphics controller that can drive a LCD or CRT displays. It has 1Gigabyte of memory (DDR-SDRAM). The ADL855PC incorporates 4 x USB 2.0 and 10/100MBit LAN which are currently in use on upgrade detailed in section 5.1.1.

Management of the sensor input, motor output, and user interface (like switch buttons, LCD, etc.) is handled by this basic processor. Basic behaviors (like obstacle avoidance) to correspond with the basic sensors are installed. The robot can be programmed in 'C' and all example code is also written in 'C' language before the robot was upgraded to ROS Indigo which will be explained in detail in section 5.1.1.

Sensors:

10 Infrared sensors: six at front, two at the sides and two at the rear. Each sensor has 3 connections (VCC, GND, O/P) but there are four wires connected to the IO module in which the 4^{th} wire is NC. There are also one set of bumper sensor at the front with 5 touch sensors and another at the rear with 2 touch sensors. The front bumper sensors detect obstacles along outside left, center left, middle, center right, and outside right and similarly rear sensors detect to their left and right. The driver written for the sensors are able to get the readings on getIR and getBumber and are briefly mentioned in the LABO-3 manual.

Actuators:

The motors power the front wheels and the back wheels are castor wheels able to move omni-directionally. The motors driver has been programmed for setting and getting its power and speed and applying brakes. Setting speed to positive moves the robot forward and vice-versa. The positive and negative sign is the indication of the

direction. Pulse-Width Modulation (PWM), Brake and Dir for each motor acts as a control to an H-bridge on the amplifier board. These signals manipulate the power or speed, the direction in which the motor turns and brake signal for its deactivation at any given point. The encoder pulse output signals are buffered and connected to the Speed signal. This is depicted in Figure 5-2 & Figure 5-3.

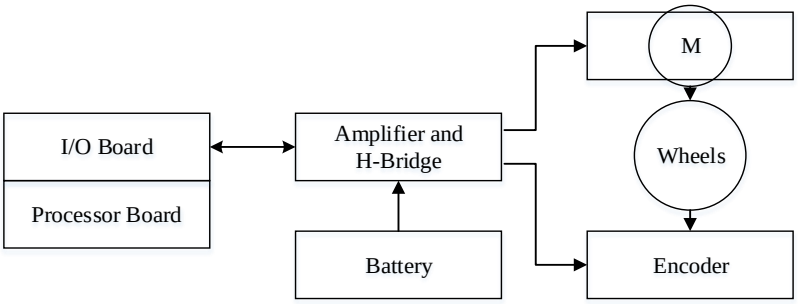

Figure 5-2 Motor Control block diagram

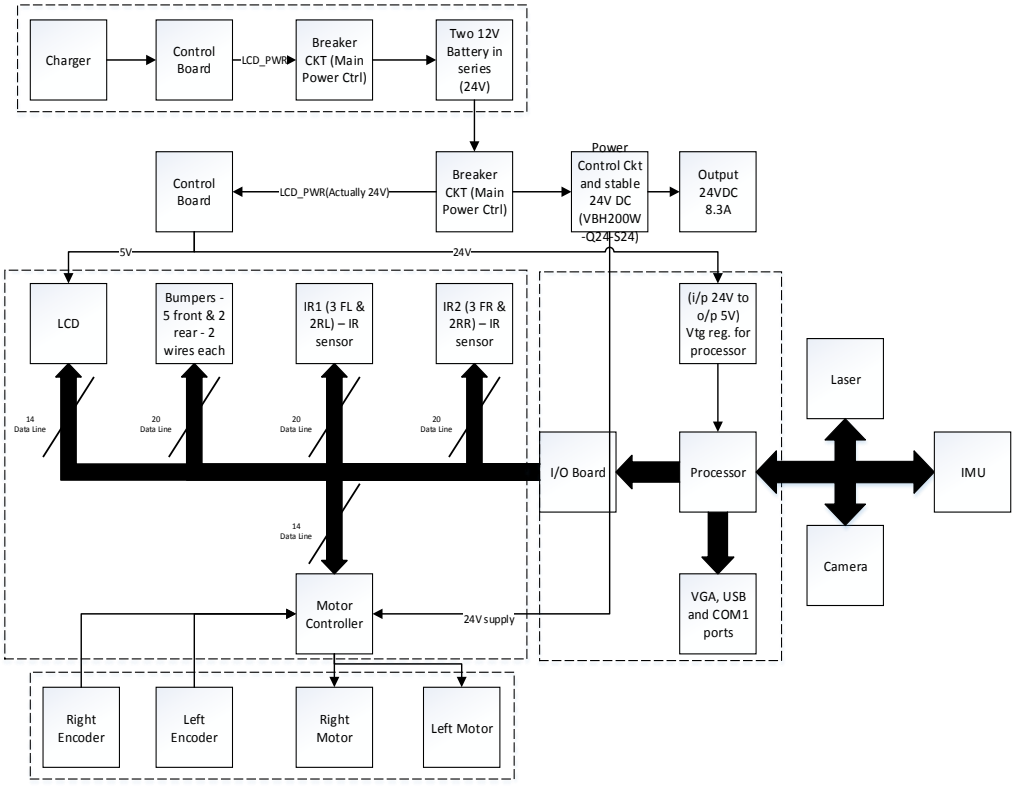

Figure 5-3 Block Diagram of the internal circuitry of LABO-3

5.1.1 Hardware upgrades

5.1.1.1 Laser scanner

URG-04LX-UG-01 scanning range finder from HOKUYO has been installed on top of the base IR sensors for the purpose of area mapping and obstacle avoidance. It has a field of view of 240 degrees and the measurement distance of 4m with an accuracy of ±30mm from 0.02m to 1m and ±3% beyond 1m. 5V 2.5W supply is enough for its working which is established from the usb – port of the ADL855 PC interface board. The scanning rate is 100ms/scan and an angular resolution of 360°/1024 steps ≈ 0.36° [35]. Based on the technical drawings of the scanner, a 3D model of it was created using SolidWorks for viewing purpose in the RVIZ and Gazebo in ROS.

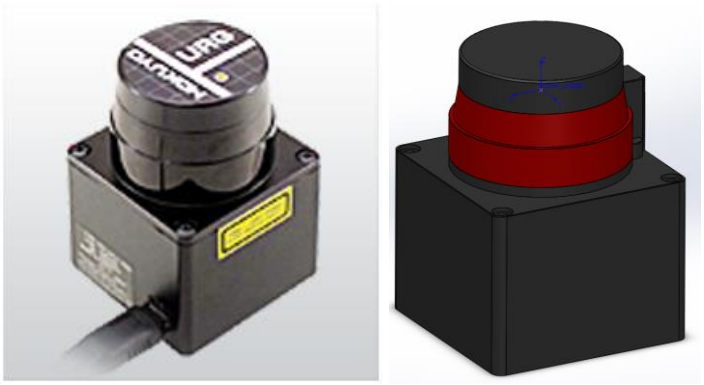

Figure 5-4 URG-04LX-UG-01 Laser scanner & its 3D solidWork model [24]

5.1.1.2 Inertial Measurement Unit

9 DOF – Razor IMU is integrated with Neptune incorporating three sensors – a gyro ITG-3200, ADXL345 accelerometer and HMC5883L magnetometer. ATmega328 is used to process the outputs of all the sensors and output over a serial interface. Considering a base IMU which reads out sensor data and would require an additional device for attitude determination which in this case is solved by having an AHRS (Attitude and heading reference system) – onboard processing system solving attitude and heading solutions. These are achieved by a form of non-linear estimation such as extended Kalman filter. A USB to TTL serial cable is used to power up the IMU and collect data serially at 57600bps. The 9DOF operates at 3.3VDC and has a down regulator to this operating voltage, hence an external voltage is not required other than the usb supply of 5VDC from the ADL855PC [36].

5.1.1.3 Camera

Asus Xtion PRO LIVE is fitted with the laser scanner for viewing purposes. It has multiple sensing functions for easy developments. It uses infrared sensors, adaptive depth detection technology, color image sensing and audio stream which can be used for various applications [23]. In my thesis, the camera has not been extensively used except

to keep track of what Neptune is seeing in front of it, but can been further used for tracking and other applications. It can be used for 3D SLAM for building a real time map of the surrounding considering the mobile robot in mind. A laser and a camera mount was designed in solidWorks for its attachment on the Neptune which was laser cut as shown in Figure 5-5.

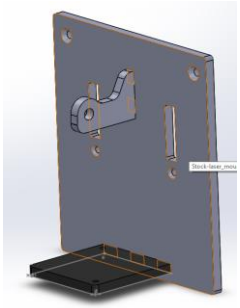

Figure 5-5 Laser and Camera mount

5.1.1.4 Wireless Router

With so many features on a mobile robot, it would be very useful to have a wireless network for communication. Asus RT-N65u router [37] was used for networking purpose. This was established so that the Neptune's performance can be viewed live while it is performing tasks. This router has 2.4GHz and 5GHz concurrent dual-band transmissions with dual processor design for stronger signals and faster connection rates up to 750Mbps combined. The router connected to the Neptune communicates data to the computers connected to its wireless network. Also for the robots connectivity to the internet without a wired connection, this router was patched with a custom firmware to work as a repeater mode [38]. This way Neptune is configured to connect to a network and also provides its own network which helps us to connect to Neptune through internet or its own network.

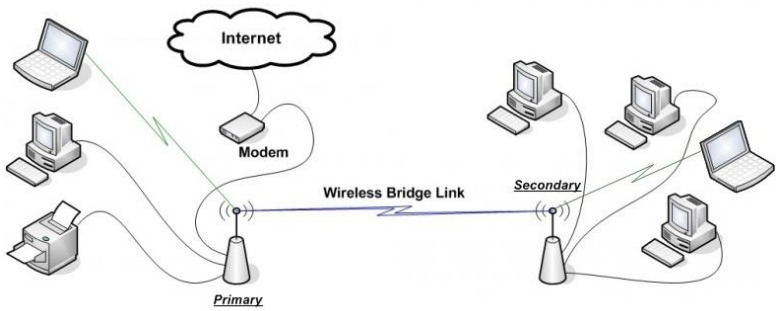

Figure 5-6 Wireless repeater mode [39]

5.1.2 Software Upgrades

5.1.2.1 RTAI patched Ubuntu 14.04 LXDE

The operating system of the Neptune was upgraded from Ubuntu 10.04 to 14.04 for its long term support. Since the computer is a single core processor unit with 1 GB RAM, a light weight environment LXDE ("Lightweight X11 Desktop Environment") was added over the Ubuntu system; optimizing it for fast performance and energy saving. For a robot's control with timing constrains the operating system is patched with RTAI – Real Time Application Interface [40] since the drivers written for the Neptune works with real time controller. After patching the OS, the input-output control of the new kernels vary and the drivers are updated for the working of the motors, LCD and the sensors. And these driver modules are initialized on start-up.

5.1.2.2 Robot Operating System (ROS)

Robot Operating System (ROS) is a flexible framework for robotic applications. It is a collection of software libraries and tools which helps simplify the robotic task across wide variety of platform. ROS encourages collaborative software development integrating multiple tools and libraries to achieve particular tasks [41]. ROS framework supports easy message passing with the use of publishers and subscribers based on message topic names. For the Neptune platform to simply the visualization of the robots movement and

to use to the hardware data in the software with the existing ROS packages, the ROS Indigo framework was integrated with Ubuntu 14.04 on Neptune. ROS framework supports C, C++ and python coding and the coding on Neptune is done in C++.

5.1.2.3 Robot Model in ROS

Odometer data estimation based on the speed of the motors running since the encoder values are buffered in the driver and speed is outputted due to irregularity in the encoder pulses. Interfaced the robot to tele-operate using keyboard, joystick and tablet interface.

The Figure 5-7 shows the model of the Neptune created in Solidworks and the extracted URDF - Unified Robot Description Format which represents a robot model used in the ROS rviz for visualization. The joints and links specified on the URDF are specific to the real robot and the motion of the joints and the robot with respect to odometry is achieved by the use of the driver written by the AAI, Inc. Canada with a further patch for it to work with the latest Ubuntu 14.04 OS. This way, the Neptune's movement can be visualized on rviz and due to the network setup, it can be operated without it being in close proximity and the visual feed captured through the integrated camera. The transformations from one joint or link to another is easily achieved in ROS by having the TF (Transform Frame) tree defined properly while creating the URDF. This is shown in the Figure 5-8 which shows the connectivity of the joints and links with respect to the odom or the base footprint frame. This makes easier for the transform listener to give the required data analysis point into any frame without having to perform manual calculation.

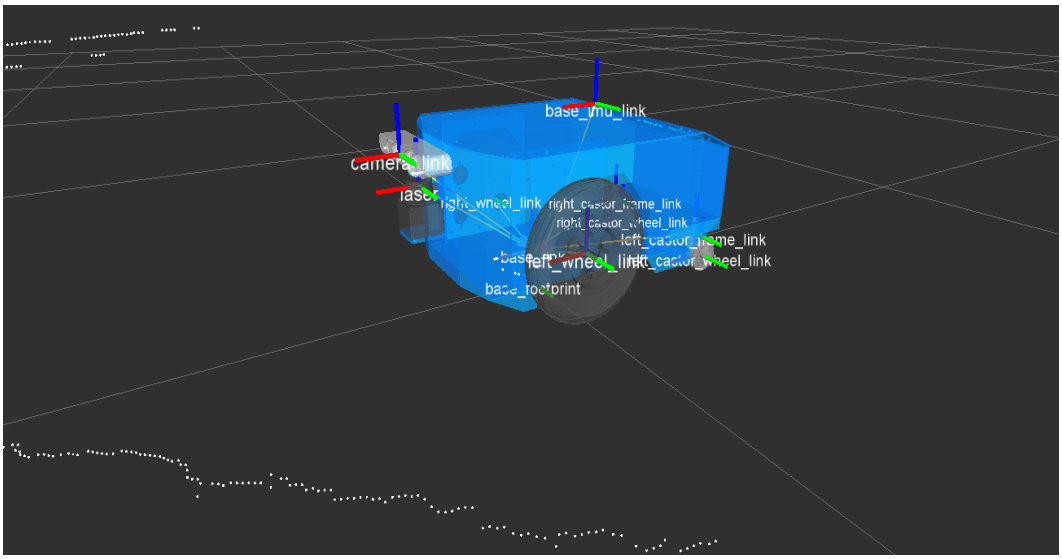

Figure 5-7 Neptune URDF model and its view on RVIZ

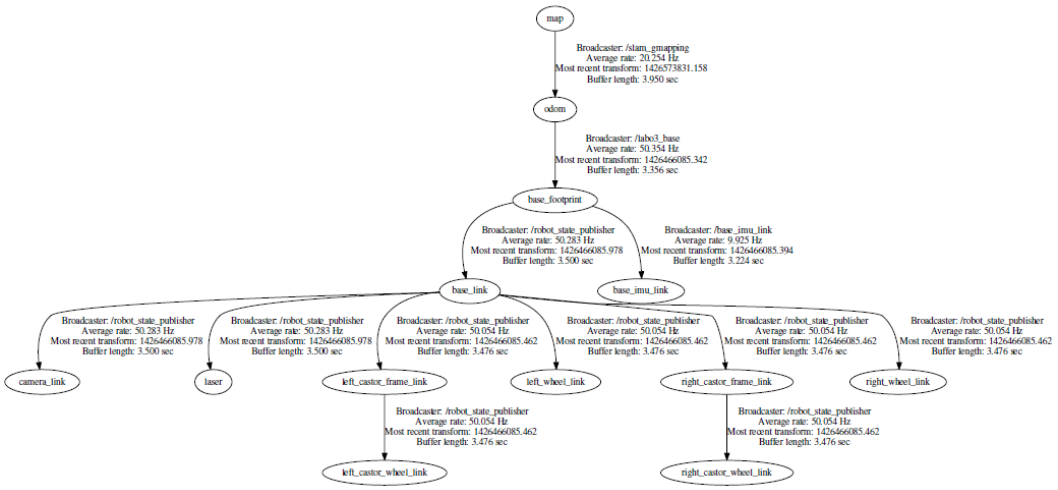

Figure 5-8 Neptune TF Tree

5.2 SLAM – Gmapping

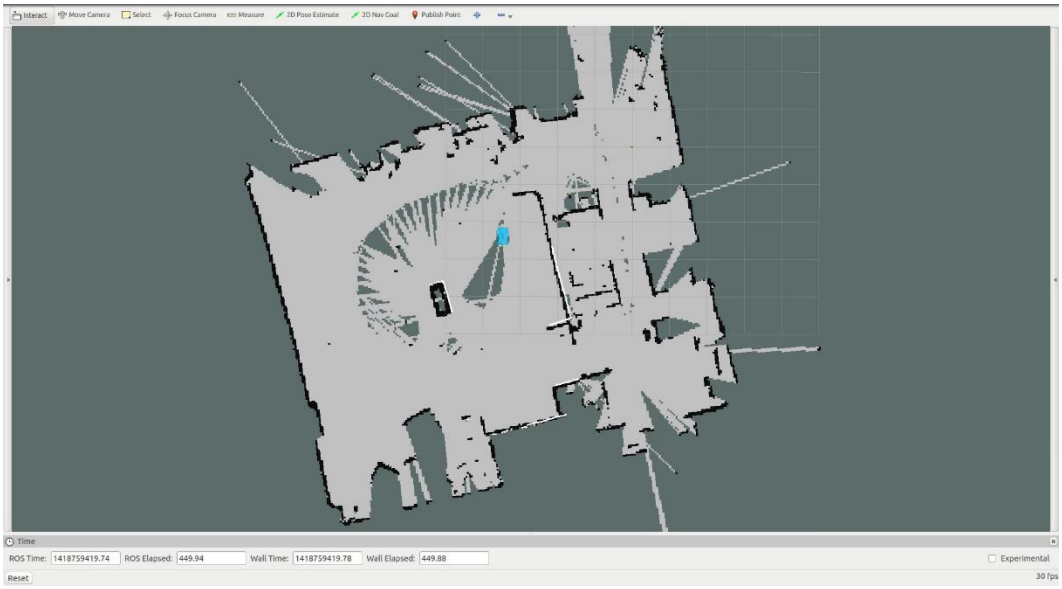

Figure 5-9 Mapping of the Lab using SLAM GMapping

The above figure is the mapped NGS lab using the Neptune operated manually through tele-op. The SLAM GMapping uses the odometry data for its pose and the laser scan data to understand the environment from which the map prediction is carried out. It keeps checking the previous map logged into the map server and updates it if there are new data points captured based on the given conditions for recording the data (Like new sampling at rotation of more than 5 degree or movement of the robot more than 0.2m).

With the navigation stack running on the Neptune, this can be achieved by goal to goal navigation avoiding obstacles autonomously. Further will discuss on the use of the navigation stack to avoid the obstacles using the Dynamic Window Approach which used the Dijikstra's or A* algorithm to achieve point navigation avoiding the obstacles with potential field around them. The Autonomous Mapping and Continuous Localization (AMCL) is used for localizing the robot once the recorded map is reloaded currently being

the static map. This follows the same principle of SLAM, however instead of mapping the environment, it compares it with the existing map and estimating the pose of the robot.

5.3 Autonomous Navigation

This section describes on how the Neptune robot is actually avoiding the obstacles. The ROS navigation stack is incorporated in Neptune with adjusting the parameters so as to satisfactorily avoid obstacles by loading the map which was saved by using GMapping technique as described in section 5.2. The trajectory planning in ROS navigation stack uses dijikstra's or A* star algorithm which calculates the cost for its travel from the current location to the goal location. The Figure 5-10 shows the setting of the goal point with a pose being set in RVIZ (ROS visualization) for the Neptune to move in the real world.

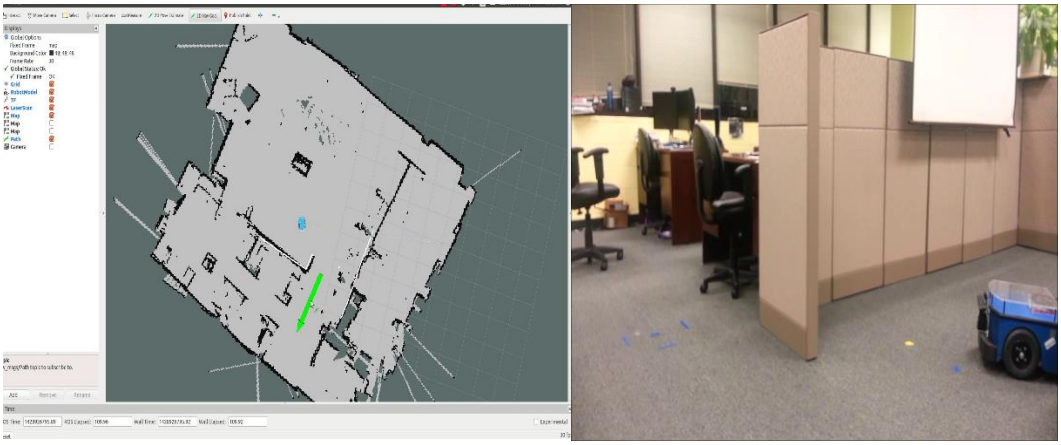

Figure 5-10 Setting Goal Points for Navigation

Then the trajectory planner of the navigation stack creates a path from its current location to the goal point based on the costs to avoid the obstacles in the way which is represented as a global planner. The local planner reflects the base movements by sending the actual command velocities for the Neptune robot to follow the trajectory path. The global planner gets updated on an interval of covering a fixed distance so that the

trajectory can be updated from its intermediate location. Since the robot does not exactly follow the traced path due to drifting odometry, the update of the global trajectory helps in unnecessary movements. Here, Autonomous Mapping and Continuous Localization (AMCL) package helps in localizing the Neptune even with drifting odometry. This package incorporates a Kalman filtering technique to estimate the robot's pose by reading the laser scanner and the odometry data. The Figure 5-11 (a) shows the global path planning avoiding the obstacle, Figure 5-11 (b) gives an intermediate location of the Neptune with an update in position using the AMCL package from where a new trajectory is calculated and Figure 5-11 (c) describes the goal point reached with the pose which was set in Figure 5-11.

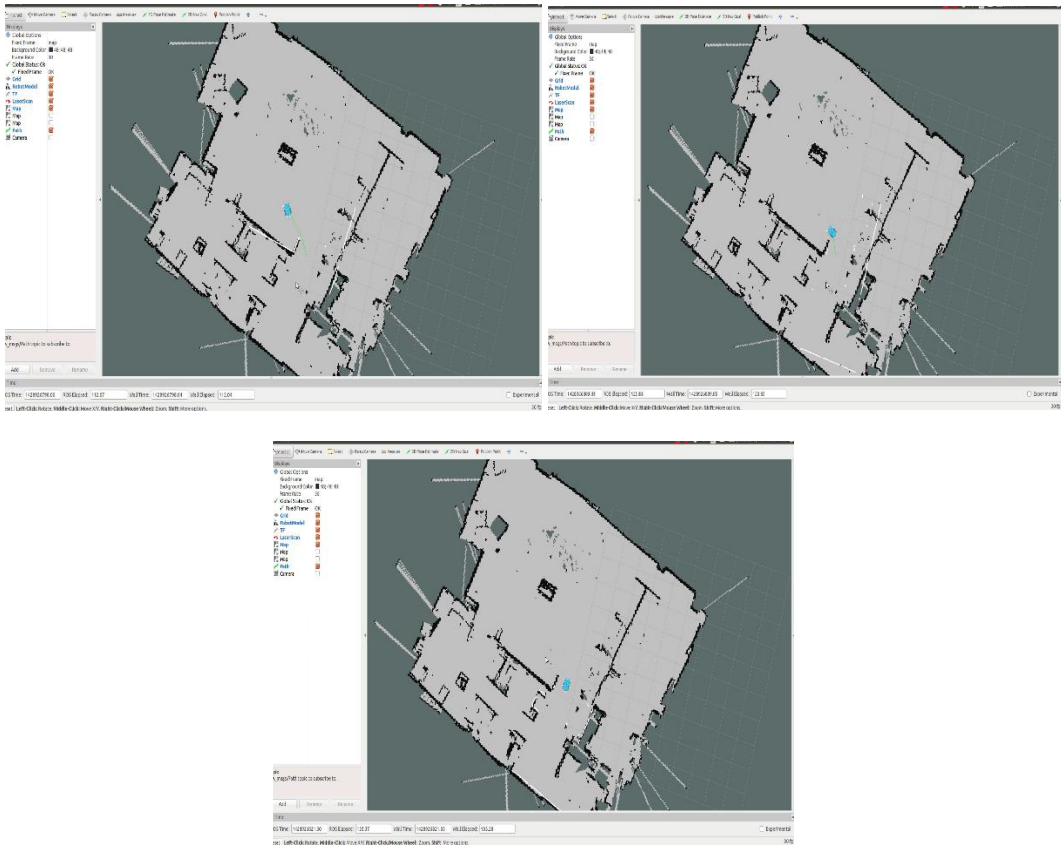

Figure 5-11 (a) Path planning using ROS Navigation Stack (b) Intermediate position with obstacle avoidance (c) Goal point reached with given pose

Chapter 6

Conclusion

This chapter summarizes the contributions of this thesis on the landmine detection challenge and put forth suggestions for future work on this topic.

6.1 Thesis Contribution

This thesis proposes an algorithm to estimate the Gaussian field parameters representing mine or metal localization using non-linear optimization techniques. A Support Vector Machine algorithm has been used to train different Gaussian metal detector signals corresponding to metals and mines to classify appropriately. A Gazebo simulator with a skid-steer platform replicating a real mine search scenario tagged with a 3-coil metal detector arm validates the parameter optimization and classification techniques.

This thesis also describes an algorithm to avoid the mines with the help of the potential field approach, by adding a repulsive field around the detected mines and has been validated in MATLAB and Gazebo simulator.

This work has also developed a ROS - capable mobile platform, Neptune, for indoor mapping, localization and autonomous navigation. The localization is carried out with the simple differential drive kinematics of the robot. The platform is upgraded with sensors with incorporation of ROS navigation stack and SLAM G-mapping which have been validated by mapping an indoor environment and autonomously navigating towards goal point avoiding obstacles.

6.2 Future research

Landmine detection is a complex real world scenario and optimizing the effectiveness of robots is still an ongoing research. This thesis discussed use of non-

linear optimization and classification algorithms on the simulated data analysis and a further research on the real kind of data sets would serve a better approach of this issue.

Further research has to be carried out on avoiding rescanning of covered areas using neural networks. More extensive analysis on the 3D mapping and autonomous navigation should be considered for the complex outdoor environment whose terrain is not flat. Adding a dynamixel arm on Neptune with a physical sensor to mimic a metal detector can help validate experimentally the proposed algorithms for the mine detection challenge in an indoor environment. Further adding a ROS-control over the Neptune robot model will provide a Gazebo model of Neptune allowing for testing of differential drive mobile robot with an arm controller to be carried out in the Gazebo simulator without the actual use of the robot.

References

[1] "What Is a Landmine?," [Online]. Available: http://www.icbl.org/en-gb/problem/what-is-a-landmine.aspx.

[2] "Anti-personnel mines: overview of the problem," [Online]. Available: https://www.icrc.org/eng/resources/documents/misc/mines-fac-cartagena-021109.htm.

[3] A. A. Berhe, "The contribution of landmines to land degradation," *Land Degradation \& Development,* vol. 18, no. 1, pp. 1-15, 2007.

[4] "Demining," [Online]. Available: http://www.un.org/en/globalissues/demining/.

[5] "MINE ACTION ENTAILS MORE THAN REMOVING LANDMINES FROM THE GROUND," [Online]. Available: http://www.mineaction.org/issues.

[6] M. K. Habib, Service robots and humanitarian demining, INTECH Open Access Publisher, 2006.

[7] A. N. Poteet, "Landmine removal: technology review and design proposal as pertaining to humanitarian demining with a focus on locomotion across soft terrain," 2008.

[8] "Researchers, officials collaborate for global demining efforts," [Online]. Available: http://www.army.mil/article/83702/Researchers__officials_collaborate_for_global_demining_efforts/.

[9] "Mine Detection Dogs," [Online]. Available: http://slnmac.gov.lk/mine-detecting-dog.

[10] A. Poling, B. Weetjens, C. Cox, N. Beyene and A. Sully, "Two strategies for landmine detection by giant pouched rats," *Journal of ERW and Mine Action,* vol. 14, 2010.

[11] "MECHANICAL DEMINING," [Online]. Available: http://www.mechanical-demining.com.

[12] M. K. Habib, "Mine clearance techniques and technologies for effective humanitarian demining," *International Journal of Mine Action,* vol. 6, no. 1, 2002.

[13] M. Hewish and R. Pengelley, "Treading a fine line: mine detection and clearance," *JANES INTERNATIONAL DEFENSE REVIEW,* vol. 30, pp. 30-48, 1997.

[14] L. Robledo, M. Carrasco and D. Mery, "A survey of land mine detection technology," *International Journal of Remote Sensing,* vol. 30, no. 9, pp. 2399-2410, 2009.

[15] J. MacDonald, J. Lockwood, J. McFee, T. Altshuler and T. Broach, "Alternatives for landmine detection," 2003.

[16] R. J. Chignell, "Ground penetrating radar-A sensor for mine detection," 1996.

[17] T. Fukuda, Y. Hasegawa, K. Kosuge, K. Komoriya, F. Kitagawa and T. Ikegami, "Environment-Adaptive Antipersonnel Mine Detection System-Advanced Mine Sweeper," in *Intelligent Robots and Systems, 2006 IEEE/RSJ International Conference on*, 2006.

[18] T. P. Montoya and G. S. Smith, "Land mine detection using a ground-penetrating radar based on resistively loaded vee dipoles," *Antennas and Propagation, IEEE Transactions on,* vol. 47, no. 12, pp. 1795-1806, 1999.

[19] R. R. Murphy, J. Kravitz, S. Stover and R. Shoureshi, "Mobile robots in mine rescue and recovery," *Robotics \& Automation Magazine, IEEE,* vol. 16, no. 2, pp. 91-103, 2009.

[20] C. Baker, A. Morris, D. Ferguson, S. Thayer, C. Whittaker, Z. Omohundro, C. Reverte, W. Whittaker, D. Hahnel and S. Thrun, "A campaign in autonomous mine mapping," in *Robotics and Automation, 2004. Proceedings. ICRA'04. 2004 IEEE International Conference on*, 2004.

[21] *Mine Safety and Health Administration - MSHA; Mine Rescue Robot.*

[22] P. G. de Santos, J. A. Cobano, E. Garcia, J. Estremera and M. Armada, "A six-legged robot-based system for humanitarian demining missions," *Mechatronics,* vol. 17, no. 8, pp. 417-430, 2007.

[23] "Humanitarian Efforts RAS-SIGHT (Special Interest Group on Humanitarian Technology)," [Online]. Available: http://www.ieee-ras.org/educational-resources-outreach/humanitarian-efforts.

[24] "CLEARPATH ROBOTICS - HUSKY," [Online]. Available: http://www.clearpathrobotics.com/husky/.

[25] "HRATC2014," [Online]. Available: http://www2.isr.uc.pt/~embedded/events/HRATC2014/Welcome.html.

[26] *The Vallon VMP3.*

[27] D. O. Popa, K. Sreenath and F. L. Lewis, "Robotic deployment for environmental sampling applications," in *Control and Automation, 2005. ICCA'05. International Conference on*, 2005.

[28] D. O. Popa, A. C. Sanderson, R. J. Komerska, S. S. Mupparapu, D. R. Blidberg and S. G. Chappel, "Adaptive sampling algorithms for multiple autonomous underwater vehicles," in *Autonomous Underwater Vehicles, 2004 IEEE/OES*, 2004.

[29] M. J. Powell, "The BOBYQA algorithm for bound constrained optimization without derivatives," *Cambridge NA Report NA2009/06, University of Cambridge, Cambridge,* 2009.

[30] P. Janik and T. Lobos, "Automated classification of power-quality disturbances using SVM and RBF networks," *Power Delivery, IEEE Transactions on,* vol. 21, no. 3, pp. 1663-1669, 2006.

[31] P. E. Stingu and F. L. Lewis, "Motion path planning for mobile robots," *target,* vol. 10, p. 10, 2007.

[32] M. F. Mysorewala, Simultaneous robot localization and mapping of parameterized spatio-temporal fields using multi-scale adaptive sampling, ProQuest, 2008.

[33] "ADL855PC - PENTIUM® M / CELERON® M CPU 1.0GHZ - 1.8GHZ," [Online]. Available: http://www.adl-usa.com/products/detail/12/adl855pc.

[34] "LABO-3 Small Size High Payload Autonomous Robot Platform," [Online]. Available: http://www.aai.ca/robots/labo3.html.

[35] "HOKUYO Photo Sensor URG-04LX-UG01," [Online]. Available: https://www.hokuyo-aut.jp/02sensor/07scanner/urg_04lx_ug01.html.

[36] "9 Degrees of Freedom - Razor IMU," [Online]. Available: https://www.sparkfun.com/products/10736.

[37] "ASUS RT-N65U Dual-Band Wireless-N750 Gigabit Router," [Online]. Available: http://www.asus.com/Networking/RTN65U/.

[38] "ASUS RT-N56U/N65U/N14U/N11P/AC51U custom firmware," [Online]. Available: https://code.google.com/p/rt-n56u/.

[39] "Wireless Bridge," [Online]. Available: http://www.dd-wrt.com/wiki/index.php/Wireless_Bridge.

[40] *RTAI - Real Time Application Interface.*

[41] *Robot Operating System.*

[42] M. W. Spong, S. Hutchinson and M. Vidyasagar, Robot modeling and control, vol. 3, Wiley New York, 2006.

[43] C. Bruschini and B. Gros, *A Survey of Research on Sensor Technology for Landmine Detection.*

[44] "ASUS - Xtion PRO LIVE," [Online]. Available: http://www.asus.com/us/Multimedia/Xtion_PRO_LIVE/.

[45] "Landmines: A Deadly Legacy," [Online]. Available: http://www.hrw.org/news/1993/09/30/landmines-deadly-legacy.

[46] K. Madsen, H. Bruun and O. Tingleff, "Methods for non-linear least squares problems," 1999.

[47] "LABO-3 Small Size High Payload Autonomous Robot Platform," [Online]. Available: http://www.aai.ca/robots/labo3.html.

Biographical Information

Sandesh Gowda received his Bachelor of Engineering in Electronics and Tele-Communications from Don Bosco Institute of Technology, Mumbai University, India in 2010 having an exposure to design RF power amplifier for audio & video transmission over a wireless channel for his graduating project. He worked in Accenture Services Pvt. Ltd. as a Software Engineering from 2010 to 2012. He then joined University of Texas at Arlington in fall 2013 (August) for his Masters in Electrical Engineering and specialization in embedded systems, control and robotics. He joined under Dr. Popa with an interest to pursue further research in mobile ground vehicles. His research include robotic deployment for landmine detection, mapping and avoidance. He worked as a research assistant at the University of Texas at Arlington Research Institute for Professor Dr. Dan Popa.